

Lectures On AdS-CFT At Weak 't Hooft Coupling At Finite Temperature

FURUUCHI Kazuyuki

Harish-Chandra Research Institute
*Chhatnag Road, Jhusi, Allahabad 211 019, India*¹
furuuchi@mri.ernet.in

Abstract

This is an introductory lecture note aiming at providing an overview of the AdS-CFT correspondence at weak 't Hooft coupling at finite temperature. The first aim of this note is to describe the equivalence of three interesting thermodynamical phenomena in theoretical physics, namely, Hawking-Page transition to black hole geometry, deconfinement transition in gauge theories, and vortex condensation on string worldsheets. The Hawking-Page transition and the deconfinement transition in weakly coupled gauge theories are briefly reviewed. Emphasis is on the study of 't Hooft-Feynman diagrams in the large N gauge theories, which are supposed to describe closed string worldsheets and probe the above equivalence. Nature of the 't Hooft-Feynman diagrams at finite temperature is analyzed, both in the Euclidean signature (the imaginary time formalism) and in the Lorentzian signature (the real time formalism). The second aim of this note is to give an introduction to the real time formalism applied to AdS-CFT.

¹Address after Aug. 2007 : National Center for Theoretical Sciences, National Tsing-Hua University, Hsinchu 30013, Taiwan, R.O.C. ; E-mail: furuuchi@phys.cts.nthu.edu.tw

Contents

1	Introduction	2
2	Hawking-Page Transition and Deconfinement at Strong Coupling	4
2.1	Euclidean path integral gravity	4
2.2	Hawking-Page transition	5
2.3	Gravity description of confinement/deconfinement in strongly coupled Yang-Mills theories	7
3	Confinement-Deconfinement Transition at Weak Coupling	11
3.1	Polyakov loop as an order parameter	11
3.2	Deconfinement transition in a toy model	12
4	't Hooft-Feynman Diagrams at Finite Temperature – Imaginary Time Formalism	15
4.1	't Hooft expansion	15
4.2	't Hooft expansion at finite temperature and Polyakov loops	17
5	't Hooft-Feynman Diagrams at Finite Temperature – Real Time Formalism	23
5.1	Motivation	23
5.2	Thermo-field dynamics	25
5.3	Path integral method in the real time formalism	27
5.4	Incorporating the effect of the confined phase background	30
5.5	The vanishing mechanism and surviving diagrams as real time closed string diagrams	33
5.6	Comments on the deconfined phase and the black hole geometry	40

1 Introduction

The AdS-CFT correspondence [1]¹ has been providing us important insights into strongly coupled gauge theories and quantum gravity. In particular, the mysterious thermodynamical nature of black holes has begun to be understood by identifying it with the dual boundary CFT at finite temperature.

If one deduce the AdS-CFT correspondence for four-dimensional CFT case from the near horizon limit of D3-branes, one obtains the relation between the radius R_{AdS} of the AdS space and the 't Hooft coupling $\lambda \equiv g_{YM}^2 N$ in the boundary Yang-Mills theory as

$$R_{AdS}^4 \propto g_{YM}^2 N l_s^4, \quad (1.1)$$

where l_s is the string length scale. In the first stage of its theoretical developments, AdS-CFT correspondence was mainly analyzed in the strong 't Hooft coupling region, where from the relation (1.1) the curvature radius of the AdS_5 is small and the supergravity approximation is valid.

Recently, weak 't Hooft coupling region also began to attract wide interests. In this case the curvature radius of the AdS_5 is around string scale, and the supergravity approximation is not valid. And we do not yet know how to quantize the string worldsheet theory on AdS space with R-R fluxes.² However, the Yang-Mills side is weakly coupled and perturbative calculation is reliable. Therefore, strategy in this region should be to extract the information of closed string theory in highly curved background from perturbative Yang-Mills analysis.³

We are particularly motivated by the two recent developments in the weak 't Hooft coupling region. One is the deconfinement transition at weak 't Hooft coupling in the large N gauge theories on S^3 [3, 4, 5, 6].⁴ The other is the Gopakumar's proposal for how

¹See [2] for a comprehensive introduction to the AdS-CFT correspondence. We will use the terminology "AdS-CFT correspondence" in a broader sense, for the duality between closed string theory on asymptotically AdS space and field theory which approaches conformal fixed point at UV. The most concrete example in mind is the duality between closed string theory on $AdS_5 \times S^5$ and $\mathcal{N} = 4$ super Yang-Mills theory.

²R-R fluxes should be there if we obtain the AdS-CFT correspondence from the near horizon limit of D3-branes.

³Since the relation (1.1) was obtained from the supergravity solution, we expect that it can be modified at weak 't Hooft coupling region where the curvature of the geometry reaches string scale. Typically, we do not trust the relation (1.1) near $\lambda = 0$, i.e. we do not assume that the closed string dual of a free Yang-Mills theory lives on the zero-radius (singular) AdS space.

⁴We are benefitted from S. Minwalla's brilliant lectures on their works.

to reorganize 't Hooft-Feynman diagrams into closed string amplitudes [7, 8, 9, 10, 11, 12, 13].⁵ This progress motivates us to seriously consider 't Hooft-Feynman diagrams in the context of AdS-CFT. Based on these two developments, we have studied the properties of 't Hooft-Feynman diagrams at finite temperature in [14, 15].⁶ This lecture note is based on these results, but we also tried to incorporate our new understandings.

In this note, we'd like to give an overview of the recent developments in the AdS-CFT correspondence in the weak 't Hooft coupling region at finite temperature. Section 2 and 3 are intended to provide sufficient materials for reading the later sections. References are provided for further learning. In section 2, after a brief introduction to the Euclidean path integral gravity, we review the Hawking-Page transition to black hole geometry, which was later identified with the deconfinement transition in the dual Yang-Mills theory via the AdS-CFT correspondence. Since the analysis is based on the Einstein-Hilbert action, it is valid in the strong 't Hooft coupling region according to (1.1). However, the existence of the transition seems robust and we expect such gravitational transition with appropriate string corrections persists up to the weak 't Hooft coupling region. In section 3, we review the deconfinement phase transition of weakly coupled large N gauge theories. Section 4 and section 5 treat the main subject of this note. In section 4, we study 't Hooft-Feynman diagrams at finite temperature in the imaginary time formalism. How to incorporate the result of section 3, namely the effect of the phase being in confinement phase or deconfinement phase, is described. This leads to the picture that the Hawking-Page transition to black hole geometry, the deconfinement transition, and vortex condensation on the closed string worldsheets are all equivalent. Making this picture clear is the first main aim of this note. In section 5, we first review the real time formalism of finite temperature theory applied to the gauge field theory. Then we describe how to incorporate the effect of the confinement/deconfinement phase background into the 't Hooft-Feynman diagrams in this case. The real time formalism corresponds to the Lorentzian signature geometry in the dual bulk theory, where the real problems in black hole physics reside. Giving an introduction to the real time formalism and explaining its application in the AdS-CFT correspondence is the second main objective of this note.

Our underlying attitude in the weak 't Hooft coupling region will be that rather than comparing the results in two sides on an equal footing, we put more weight on the Yang-

⁵See the references therein and in [14] for other approaches to obtain closed string amplitudes from perturbative Yang-Mills theories.

⁶R. Gopakumar first suggested us to pursue his project in the finite temperature case. We would like to thank him for the collaboration in the early stage of [14] as well as many insightful suggestions.

Mills side. We will mostly start from the perturbative Yang-Mills theory and try to read off or “define” the concepts in the bulk.

2 Hawking-Page Transition and Deconfinement at Strong Coupling

In this section we briefly review the Hawking-Page transition [16], a thermal phase transition to a black hole geometry in asymptotically AdS space. This was identified as the dual description of the deconfinement transition in Yang-Mills theories through the AdS-CFT correspondence in [17, 18].

2.1 Euclidean path integral gravity

The partition function for canonical ensemble in a quantum field theory is given by

$$Z = \text{Tr} \left\{ e^{-\beta \hat{H}(\hat{\phi}, \hat{\pi})} \right\}, \quad (2.1)$$

where Tr is the trace in the Hilbert space and \hat{H} is the Hamiltonian of the system of interest. β is the inverse temperature. $\hat{\phi}$ is a field operator and $\hat{\pi}$ is its conjugate momentum. By following the usual steps from canonical quantization to path integral, we can rewrite (2.1) as

$$Z = \int \mathcal{D}\phi e^{-\int_0^\beta d\tau \mathcal{L}(\phi)}, \quad (2.2)$$

where ϕ denotes the path integral counterpart of the field operator appearing in the (2.1), and \mathcal{L} is the Lagrangian.⁷ Since compared with the usual time translation operator $e^{i\hat{H}t}$, β in $e^{-\beta\hat{H}}$ can be seen as imaginary time direction, this formalism is called imaginary time formalism. It is also called Euclidean time formalism because the rotation from the real time to the imaginary time brings one from the Lorentzian time signature to the Euclidean time signature. In rewriting (2.1) to (2.2), it follows that bosonic fields ϕ_B obey the periodic boundary condition

$$\phi_B(\tau + \beta) = \phi_B(\tau), \quad (2.3)$$

and fermionic fields ϕ_F obey the anti-periodic boundary condition

$$\phi_F(\tau + \beta) = -\phi_F(\tau). \quad (2.4)$$

⁷We have assumed that the Hamiltonian depends on the canonical momenta in a standard manner and they have been integrated out.

In the case of gravity, we do not have satisfactory formalism for canonical quantization yet. However, we may just assume its existence and start from the Euclidean path integral (2.2), and take the classical approximation [19]. Then we obtain

$$Z \simeq e^{-I(\phi_{cl})}, \quad (2.5)$$

where ϕ_{cl} is a classical solution of the equation of motion with appropriate conditions imposed by the system of interests, e.g. static, spherically symmetric and so on.⁸

2.2 Hawking-Page transition

Now we use the Euclidean path integral formalism in the case of the asymptotically AdS space.⁹ The model action we study here is

$$I = -\frac{1}{16\pi G_N} \int d^5x \sqrt{g} \left\{ R + \frac{12}{b^2} \right\}. \quad (2.6)$$

Here, G_N is the five-dimensional Newton's constant. In the case of the near horizon geometry of D3-branes, constant flux plays the role of the cosmological constant in (2.6), and we get the similar results. For a solution of the equation of motion, $R_{\mu\nu} - \frac{1}{2}Rg_{\mu\nu} - \frac{1}{2}\frac{12}{b^2}g_{\mu\nu} = 0$, the value of the action becomes

$$I = \frac{1}{2\pi G_N b^2} \int d^5x \sqrt{g}, \quad (2.7)$$

that is, the volume of the space-time times $\frac{1}{2\pi G_N b^2}$.¹⁰ The AdS metric is a solution to the equation. In the global coordinates, it is given by

$$ds^2 = \left(1 + \frac{r^2}{b^2}\right) d\tau^2 + \left(1 + \frac{r^2}{b^2}\right)^{-1} dr^2 + r^2 d\Omega_3^2, \quad (2.8)$$

where $d\Omega_3^2$ is a usual metric on S^3 . The τ direction is periodically identified to discuss canonical ensemble (the thermal circle). To discuss canonical ensemble in gravity, one first needs to choose which direction to be the Euclidean time, or equivalently should choose the Hamiltonian. Our choice is to use the τ direction in the coordinate (2.8). With this choice, the asymptotic boundary at ($r \rightarrow \infty$) becomes $S^1 \times S^3$ (up to a diverging overall factor which we rescale). Therefore, the dual Yang-Mills theory lives on the spatial

⁸When there are multiple solutions, we sum over contributions from all those, or may take the absolute minimum as the leading contribution.

⁹Here we are following the $n = 4$ case of section 2.4 of [18].

¹⁰The action additionally has a surface term [19], but this vanishes for the AdS-Schwarzschild black hole solution because the difference between it and the AdS space vanishes too rapidly at infinity [16].

manifold S^3 . We are interested in the static spherically symmetric configurations. Above certain temperature which will be described shortly, there is another solution. It is the AdS-Schwarzschild black hole geometry whose metric is given by

$$ds^2 = \left(1 + \frac{r^2}{b^2} - \frac{\omega_4 M}{r^2}\right) d\tau^2 + \left(1 + \frac{r^2}{b^2} - \frac{\omega_4 M}{r^2}\right)^{-1} dr^2 + r^2 d\Omega_3^2, \quad (2.9)$$

where

$$\omega_4 \equiv \frac{16\pi G_N}{3\text{Vol}(S^3)}, \quad (2.10)$$

and M is the mass of the black hole. In the Euclidean time signature, the space-time is restricted to the region $r \geq r_+$, where r_+ is the largest solution to the equation

$$1 + \frac{r^2}{b^2} - \frac{\omega_4 M}{r^2} = 0. \quad (2.11)$$

In the Lorentzian signature counterpart, r_+ becomes the location of the black hole event horizon. Therefore, the Euclidean geometry only covers the region outside the horizon. In the Euclidean path integral gravity, temperature of the black hole is determined from the requirement that there should be no conical singularity at the horizon $r = r_+$. This determines the period β_0 of the τ coordinate to be

$$\beta_0 = \frac{2\pi b^2 r_+}{2r_+^2 + b^2}. \quad (2.12)$$

From the AdS-CFT point of view, a geometry with a conical singularity is not exactly the saddle point for a given temperature and hence excluded.

The classical action for the above solutions, or the space-time volume which is proportional to it, is infinite so we need to regularize it. We put a cut-off R in the radial direction r . Then, the volume of the AdS space is given by

$$V_1(R) = \int_0^{\beta'} d\tau \int_0^R dr \int_{S^3} r^3. \quad (2.13)$$

And for the AdS-Schwarzschild black hole, it is

$$V_2(R) = \int_0^{\beta_0} d\tau \int_{r_+}^R dr \int_{S^3} r^3. \quad (2.14)$$

We are interested only in the difference of the two actions. To compare the two, we match the physical circumference of the Euclidean time direction at R . This determines β' as

$$\beta' \sqrt{\frac{R^2}{b^2} + 1} = \beta_0 \sqrt{\frac{R^2}{b^2} + 1 - \frac{\omega_4 M}{R^2}}. \quad (2.15)$$

Then, the difference of the action for the two solutions is calculated as

$$I = \frac{1}{2\pi G_N b^2} \lim_{R \rightarrow \infty} (V_2 - V_1) = \frac{\text{Vol}(S^3)(b^2 r_+^3 - r_+^5)}{4G_N(4r_+^2 + 2b^2)}. \quad (2.16)$$

The action becomes negative at $r_+ \geq b$, or equivalently $\beta_0 \leq \frac{2\pi}{3}b$, and the phase transition to the AdS-Schwarzschild black hole geometry takes place. Then the energy of the AdS-Schwarzschild black hole geometry is given by

$$E = \frac{\partial I}{\partial \beta_0} = \frac{\text{Vol}(S^3)3(r_+^4 - r_+^2 b^2)}{16\pi G_N b^2} = M, \quad (2.17)$$

and the entropy is given by

$$S = \beta_0 E - I = \frac{1}{4G_N} r_+^4 \text{Vol}(S^3) = \frac{A}{4G_N}, \quad (2.18)$$

where A is the area of the horizon.

Actually, there are two black hole solutions for given $\beta_0 < \frac{\pi}{\sqrt{2}}b$. Here, we are interested in the absolute minimum of the classical action. This corresponds to choosing the larger solution for r_+ for given β_0 in (2.12). The larger r_+ solution is often called big black hole, when compared with the smaller r_+ solution which is often called small black hole. The small black hole has negative specific heat and hence unstable. It reduces to the familiar Schwarzschild black hole in flat space in the $b \rightarrow$ limit. (For the big black hole, r_+ becomes infinite in the $b \rightarrow$ limit, so there is actually no finite flat space limit.) We only consider the classical minimum of the action in our saddle point approximation, i.e. the big black hole in the high temperature phase.

2.3 Gravity description of confinement/deconfinement in strongly coupled Yang-Mills theories

Witten has given some gravity descriptions for expected phenomena in strongly coupled Yang-Mills theory [17, 18]. Here we will recall few of them which are most relevant for us in the later discussions.

One of the order parameters for the deconfinement is the action itself. In the large N expansion in Yang-Mills theory, the action scales like $O(N^0)$ in the confined phase and $O(N^2)$ in the deconfined phase. In the gravity side, the action scales like $1/G_N \sim 1/g_s^2$ (g_s is the closed string coupling) in the black hole phase which corresponds to the deconfined phase. This matches with the Yang-Mills side via the identification of the 't Hooft expansion with the genus (loop) expansion of the closed string theory (section 4).

Another important order parameter is the expectation value of the Polyakov loop, or the Wilson loop wrapping around the Euclidean time direction, defined by

$$\mathcal{P} \equiv \frac{1}{N} \text{tr} P e^{i \int_0^\beta d\tau A_0}, \quad (2.19)$$

where P denotes the path ordering. We will explain more about the Polyakov loop in Yang-Mills theory in the next section. In the bulk side in the classical gravity approximation, the expectation value of the Wilson loop is calculated from the (regularized) area of the minimal surface ending on the loop [20, 21, 22, 23] (see also [2, 24] for a learning):¹¹

$$\langle \mathcal{P} \rangle \sim e^{-T_{st} \mathcal{A}}, \quad (2.20)$$

where \mathcal{A} is the area of the minimal surface in the bulk ending on the loop and T_{st} is the tension of fundamental string. As we will explain in the next section, in the confined phase the expectation value of the Polyakov loops vanishes. In the dual gravity side, this is explained as follows. The thermal AdS geometry (the AdS geometry periodically identified in τ -direction) has a topology $S^1 \times B^4$ (B^4 stands for the four-dimensional ball), and there is a non-contractible circle wrapping in the thermal circle S^1 , see Fig.1. This prevents the worldsheet with a disk topology to end on the thermal circle at the boundary. This means that the Polyakov loop expectation value is zero at the closed string tree level, or in the $N \rightarrow \infty$ limit. Thus the thermal AdS geometry corresponds to the confined phase. On the other hand, for the AdS-Schwarzschild black hole geometry has a topology of $R^2 \times S^3$, and hence there's no non-contractible circle, see Fig.2. In this case, a worldsheet with a disk topology can end on the thermal circle on the boundary. Then the (regularized) area of the surface gives the Polyakov loop expectation value. Therefore, the AdS-Schwarzschild black hole geometry should correspond to the deconfined phase where the Polyakov loops have expectation values.

If one compares the AdS-Schwarzschild black hole geometry (2.9) with the AdS geometry (2.8), one notices that in the black hole geometry the space-time beyond the horizon $r = r_+$ looks as disappeared. It is well known that a closed string winding around a circle with anti-periodic boundary conditions for fermions becomes tachyonic when the circle

¹¹Precisely speaking, what is calculated in this way is a generalization of the Wilson loop including scalar fields [21]. However, in the low temperature limit, all fields other than A_0 on S^3 become massive if dimensionally reduced and the generalized Wilson loop reduces to the conventional one at low energy. On the other hand, in the high temperature limit those fields are expected to acquire a mass of a scale given by the temperature, and at distance much longer than that the generalized Wilson loop again reduces to the conventional one.

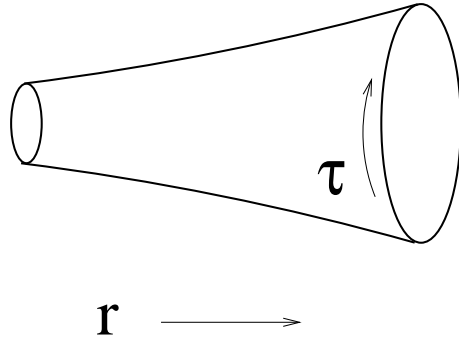


Figure 1: The topology of the thermal AdS geometry. τ and r directions are depicted.

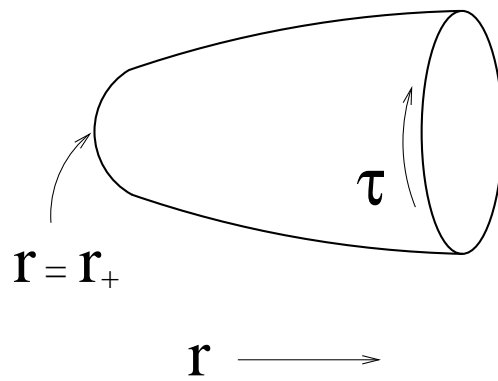


Figure 2: The topology of the AdS-Schwartzchild geometry.

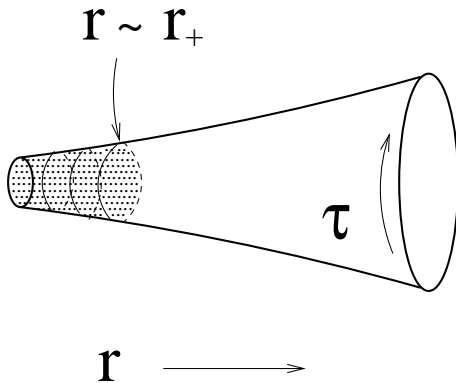


Figure 3: At certain temperature, the radius of the thermal circle reaches string scale in the region beyond $r \sim r_+$. The space-time becomes unstable due to the closed string winding tachyon condensation, and expected to decay to “no-space-time” phase. The endpoint is expected to be the AdS-Schwarzschild geometry Fig.2.

shrinks to the string scale [25]. It has been argued that the above change of the space-time geometry is caused by condensation of such tachyonic closed string.¹² Analogous to the open string tachyon condensation to “no-D-brane” vacuum [26], the condensation of the closed string tachyon was speculated to lead to the “no-space-time” phase and eliminate the space-time beyond $r \sim r_+$ [27, 28, 29, 30, 31, 32, 33]. We will explore more on this point from the Yang-Mills side using the AdS-CFT correspondence.

From the next section we will analyze weakly coupled Yang-Mills theories. Since the analysis in this section is based on the Einstein-Hilbert action, it is valid in the strong 't Hooft coupling region, according to the relation between the 't Hooft coupling and the curvature radius of the AdS (1.1). However, the existence of the confinement-deconfinement transition seems robust in the Yang-Mills side, and therefore we expect that this kind of gravitational phase transition persists with appropriate string corrections, all the way up to the weak 't Hooft coupling region. Although the detailed form of the metric will be modified, we expect that general features like the difference of topology in two geometries remain the same.¹³

¹²Clarifying comment: When the order of the phase transition is first order, generically (though it depends on the shape of the potential for the winding mode) the phase transition takes place before the tachyonic mode appears. In other words, when the phase transition takes place, the winding mode is still not tachyonic in the thermal AdS geometry.

¹³See [34] for an investigation of a limit where both Yang-Mills side and string theory side are weakly coupled.

3 Confinement-Deconfinement Transition at Weak Coupling

3.1 Polyakov loop as an order parameter

We will study the gauge theory action in which all fields are in the adjoint representation of the $SU(N)$ gauge group. To discuss canonical ensemble, the Euclidean time direction is compactified to a thermal circle with the circumference β . The generator of the gauge transformation should satisfy

$$g(\tau + \beta) = g(\tau), \tag{3.1}$$

in order not to change the boundary conditions for the fields. However, since all the fields are in the adjoint representation, they transform trivially under the center of the gauge group. In this case we can consider more general transformation

$$g(\tau + \beta) = g(\tau)h, \tag{3.2}$$

where h is an element of the center of the gauge group which can be identified with the N -th root of unity $e^{2\pi i \frac{n}{N}}$, $n = 1, \dots, N - 1$.

An order parameter for the Z_N symmetry is given by the expectation value of the Polyakov loop defined by

$$\mathcal{P} \equiv \frac{1}{N} \text{tr} P e^{i \int_0^\beta d\tau A_0}, \tag{3.3}$$

where P denotes the path ordering and tr is the trace in the fundamental representation of the gauge group. Physically, the Polyakov loop \mathcal{P} measures the exponential of the free energy for adding an external source quark (a field in the fundamental representation of the $SU(N)$ gauge group). In the confined phase, adding an external quark source costs infinite free energy, and thus the expectation value of the Polyakov loop is zero. To be more precise, actually on a compact space like S^3 , due to the Gauss's law constraints the expectation value of the single Polyakov loop is automatically zero. However, the way it becomes zero is different in the confined phase and the deconfined phase. In the confined phase a single large N saddle point (see below) gives zero whereas in the deconfined phase each saddle points gives non-zero value but the sum over the N saddle points related by the Z_N symmetry gives zero. It is not difficult to construct a related order parameter which probes the phase on the compact space. The operator $\langle |\mathcal{P}|^2 \rangle$ which amounts to adding external quark and anti-quark, can do the job.¹⁴

¹⁴See [35] for more about the Z_N symmetry in AdS-CFT.

For later purpose, we also define a straightforward generalizations of the Polyakov loop, the Wilson loops wrapping around the thermal circle for n times:

$$\mathcal{P}_n \equiv \frac{1}{N} \text{tr} P e^{i \int_0^{n\beta} d\tau A_0}. \quad (3.4)$$

We will also call these as Polyakov loops.

Usually, there's no phase transition in a field theory on a compact spatial manifold. However, if one takes the size of the gauge group N to infinity, the large N phase transition can take place [36, 37, 38].

Now suppose we have a partition function of a theory with fields ϕ^i coupled to the gauge field:

$$Z = \int \mathcal{D}A_0 \int \mathcal{D}\phi^i e^{-S(A_0, \phi^i)}. \quad (3.5)$$

To determine whether the confined phase or the deconfined phase is realized, we integrate over all the massive fields which¹⁵ to obtain the effective action $S_{eff}(A_0)$ for the temporal component of the gauge field A_0 :

$$Z = \int \mathcal{D}A_0 e^{-S_{eff}(A_0)}. \quad (3.6)$$

The phase can be known by calculating the expectation values of the Polyakov loops like

$$\langle |\mathcal{P}|^2 \rangle = \int \mathcal{D}A_0 |\mathcal{P}|^2 e^{-S_{eff}(A_0)}, \quad (3.7)$$

as explained above.

3.2 Deconfinement transition in a toy model

Now we present an explicit toy model example.¹⁶ This toy model still captures the essential points of the confinement-deconfinement phase transition of the large N gauge theories on S^3 at weak coupling, which we are interested in. The action we will consider is

$$S = \int_0^\beta d\tau \text{tr} \frac{1}{2} (D_0 \Phi^i D_0 \Phi^i + \omega^2 \Phi^2) \quad (i = 1, \dots, d). \quad (3.8)$$

We assume that ω^2 is positive (non-zero) since that is the case if one does similar calculations in Yang-Mills theories on S^3 .

¹⁵In the cases we will be interested in the later section, there are no massless fields.

¹⁶The explanations in this subsection is based on [39].

We can choose the gauge in which A_0 is constant and diagonal:

$$\frac{\partial}{\partial \tau} A_0 = 0, \quad A_{0ab} = \delta_{ab} A_a. \quad (3.9)$$

However one cannot gauge away the constant mode of A_0 when the Euclidean time is compactified on a circle. Recall (3.1). A shift of an eigen-value A_a by $2\pi/\beta$ can be canceled by the gauge transformation of the form $g(\tau) = \text{diag}(1, \dots, 1, e^{\frac{2\pi i}{\beta}\tau}, 1, \dots, 1)$ which is periodic: $g(\tau + \beta) = g(\tau)$, and thus is a legitimate gauge transformation. Therefore the eigen-values A_a live on a circle with radius $1/\beta$.

The Faddeev-Popov determinant for the first of the gauge fixing conditions (3.9) is

$$\det' \left(-\frac{d}{d\tau} \left(-\frac{d}{d\tau} + i(A_a - A_b) \right) \right). \quad (3.10)$$

The prime on the det means that the zero-mode of the time derivative is omitted from the determinant. The Faddeev-Popov determinant for the diagonalization of the gauge field is the familiar Vandermonde determinant:

$$\prod_{a \neq b} (A_a - A_b). \quad (3.11)$$

Combining them together, we obtain

$$\det' \left(-\frac{d}{d\tau} \right) \det \left(-\frac{d}{d\tau} + i(A_a - A_b) \right). \quad (3.12)$$

Using the formula

$$\det \left(-\frac{d}{d\tau} + \omega \right) = 2 \sinh \frac{\beta\omega}{2} \quad (3.13)$$

for the periodic boundary conditions, we obtain

$$Z = \int \prod_{a=1}^N dA_a \prod_{a \neq b} \sin \frac{\beta}{2} |A_a - A_b| \prod_{a \neq b} \left(\frac{1}{\sinh \left(\frac{\beta}{2} (\omega + i(A_a - A_b)) \right)} \right)^d. \quad (3.14)$$

Thus in this case we obtain the following effective action for A_0 :

$$\begin{aligned} S_{eff}(A_0) &= \sum_{a \neq b} d \ln \left(\sinh \left(\frac{\beta}{2} (\omega + i(A_a - A_b)) \right) \right) - \ln \sin \frac{\beta}{2} |A_a - A_b|. \end{aligned} \quad (3.15)$$

In the large N limit, S_{eff} is order $O(N^2)$, so we can apply the saddle point method. We define the eigen-value density $\rho(\theta)$ by

$$\rho(\theta) \equiv \frac{1}{N} \sum_{a=1}^N \delta(\theta - \beta A_a), \quad (3.16)$$

where we can set $-\pi \leq \theta \leq \pi$ without loss of generality. $\rho(\theta)$ is normalized as

$$\int_{-\pi}^{\pi} d\theta \rho(\theta) = 1. \quad (3.17)$$

Since $\rho(\theta)$ is a density, it also satisfies

$$\rho(\theta) \geq 0. \quad (3.18)$$

Using the eigen-value density $\rho(\theta)$, (3.15) can be rewritten as

$$\begin{aligned} S_{eff} &= N^2 \int_{-\pi}^{\pi} d\theta \int_{-\pi}^{\pi} d\theta' \rho(\theta) \rho(\theta') \left\{ d \ln \left(\sinh \left(\frac{\beta\omega}{2} + \frac{i}{2}(\theta - \theta') \right) \right) - \ln \left(\sin \frac{1}{2} |\theta - \theta'| \right) \right\}. \end{aligned} \quad (3.19)$$

It is instructive to Fourier expand the eigen-value density $\rho(\theta)$:

$$S_{eff} = N^2 \sum_{n=1}^{\infty} \rho_n \rho_{-n} \frac{1 - de^{-n\beta\omega}}{n}, \quad (3.20)$$

where

$$\rho_n \equiv \int_{-\pi}^{\pi} d\theta \rho(\theta) e^{in\theta} = \frac{1}{N} \sum_{a=1}^N e^{in\beta A_a} = \frac{1}{N} \text{tr} U^n. \quad (3.21)$$

Thus the n -th Fourier mode ρ_n is nothing but the Polyakov loop \mathcal{P}_n in (3.4) which wind around the thermal circle n times. We obtain the saddle point equation from (3.19):

$$\int d\theta' \rho(\theta') i \coth \left(\frac{\beta\omega}{2} + \frac{i}{2}(\theta - \theta') \right) = \int d\theta' \rho(\theta') \cot \frac{1}{2}(\theta - \theta'), \quad (3.22)$$

where it is understood that the principal value around the singularity is taken in the integral on the right hand side.

The homogeneous eigen-value density distribution $\rho(\theta) = \frac{1}{2\pi}$ is always a solution to the saddle point equation (3.22). Since the Polyakov loop expectation values vanish in this case, it corresponds to the low temperature confined phase.

As we increase the temperature, from (3.20) one sees that at $\beta = \beta_c \equiv \frac{\ln d}{\omega}$ the $n = 1$ mode becomes unstable. This leads to the deconfinement phase transition. It may be worthwhile to note that the transition does not occur at finite temperature in the $d = 1$ case. (This can be seen from the fact that for $d = 1$ the density of gauge singlet states doesn't show the Hagedorn behavior [3, 4, 5, 39].)

One might have felt little bit odd that there is a confined phase in the weakly coupled gauge theory. When one discusses about the strength of the coupling, one uses canonically

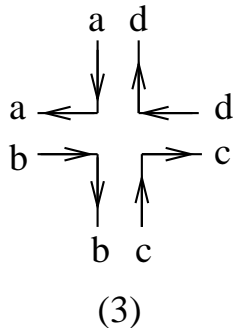
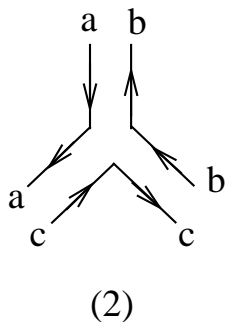
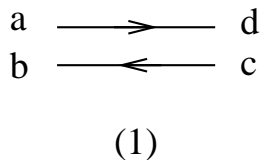


Figure 4: (1) is the propagator $\langle \Phi_{ab} \Phi_{cd} \rangle$. (2) and (3) schematically denote the interaction vertices, just showing how the flow of the matrix indices are drawn.

normalized fields. However, the constant mode of A_0 does not have a kinetic term, and therefore it is always strongly coupled, even when one takes the 't Hooft coupling small.

For further readings for how to determine the eigen-value distributions in the high temperature phase, see [40]. For the study of Yang-Mills theories on S^3 , which is of our actual interest, see [5, 6, 41].

4 't Hooft-Feynman Diagrams at Finite Temperature – Imaginary Time Formalism

4.1 't Hooft expansion

Let us consider a lagrangian of the form

$$\mathcal{L}(\Phi^i) = \frac{1}{g_{YM}^2} \text{tr} \left\{ \partial_\mu \Phi^i \partial_\mu \Phi^i + V(\Phi^i) \right\}, \tag{4.1}$$

where Φ_{ab}^i are fields in the adjoint representation of the $SU(N)$ gauge group.¹⁷ 't Hooft noticed that if one takes the large N limit $N \rightarrow \infty$ together with $g_{YM} \rightarrow 0$ ¹⁸ with the 't

¹⁷We will neglect the subleading differences in $1/N$ between $SU(N)$ and $U(N)$ gauge group in the discussion here.

¹⁸For the $\mathcal{N} = 4$ super Yang-Mills theory, the coupling does not run. In general the coupling runs and this expansion becomes formal. However on a compact manifold S^3 , if we set the size of its radius R

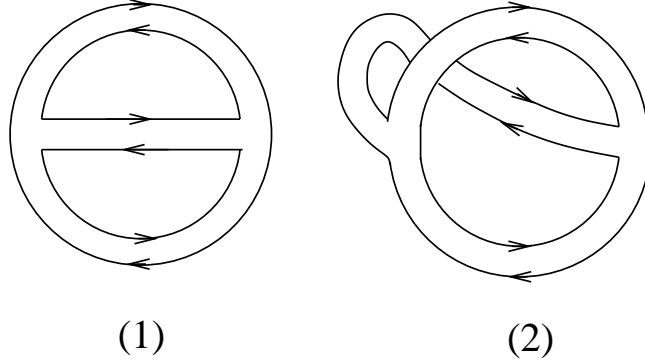


Figure 5: Examples of 't Hooft-Feynman diagrams. (1) can be drawn on a sphere (genus zero surface) whereas (2) can be drawn on a torus (genus one surface) (try).

Hooft coupling $\lambda \equiv g_{YM}^2 N$ held fixed, Feynman diagrams of such theories are organized into simplicial decompositions of Riemann surfaces [42]. To see this, we explicitly follow the flow of the matrix indices using the 't Hooft's double line notation depicted in Fig.4. Then, for a given Feynman diagram, each interaction vertex contributes by a factor of $1/g_{YM}^2 = N/\lambda$, and each propagator contributes by a factor of λ/N , and each index loop contributes by a factor N since it contains a sum over N gauge indices. Therefore, a diagram with V vertices (vertices of the simplicial decomposition of the surface on which the diagram can be drawn), E propagators (edges of the simplicial decomposition) F index loops (faces of the simplicial decomposition) contributes with a factor

$$N^{V-E+F} \lambda^{E-V} = N^\chi \lambda^{E-V}, \quad (4.2)$$

where $\chi \equiv V - E + F$ is the Euler character of the surface on which the diagram can be drawn. It is $\chi = 2 - 2g$ for closed oriented surface with genus g (the number of handles).¹⁹ Therefore, if we identify the Riemann surfaces with closed string worldsheets, the closed string coupling is read as

$$g_s \propto \frac{1}{N}. \quad (4.3)$$

to be much smaller than the scale Λ_{QCD} dynamically generated from the asymptotically free Yang-Mills theory, i.e. $R\Lambda_{QCD} \ll 1$, the 't Hooft limit makes sense.

¹⁹Here we are discussing connected diagrams. For disconnected diagrams we have such contributions from each connected component.

4.2 't Hooft expansion at finite temperature and Polyakov loops

Now we study the perturbative expansion around the saddle points of A_0 discussed in section 3. The covariant derivative for adjoint fields is given by

$$D_0\Phi(\tau) = \partial_0\Phi(\tau) - i[A_0, \Phi(\tau)]. \quad (4.4)$$

We have suppressed the spatial dependence cause it is not essential in the following discussions. Bosonic fields obey the periodic boundary condition

$$\Phi(\tau + \beta) = \Phi(\tau). \quad (4.5)$$

(One can make similar arguments for fermionic fields.) It is convenient to make a field redefinition

$$\tilde{\Phi}(\tau) = e^{-iA_0\tau}\Phi(\tau)e^{iA_0\tau}. \quad (4.6)$$

Then the covariant derivative is transformed into normal derivative:

$$\partial_0\tilde{\Phi}(\tau) = e^{-iA_0\tau}D_0\Phi(\tau)e^{iA_0\tau} \quad (4.7)$$

And the boundary condition for $\tilde{\Phi}(\tau)$ becomes

$$\tilde{\Phi}(\tau + \beta) = U^{-1}\tilde{\Phi}(\tau)U, \quad (4.8)$$

where

$$U \equiv e^{i\beta A_0}. \quad (4.9)$$

The propagator on $S^1 \times S^3$ can be obtained from the propagator on $R \times S^3$ by the method of images:

$$\langle \tilde{\Phi}_{ab}(\tau)\tilde{\Phi}_{cd}(0) \rangle_{S^1 \times S^3} = \sum_{n=-\infty}^{\infty} \langle (U^{-n}\tilde{\Phi}(\tau + n\beta)U^n)_{ab}\tilde{\Phi}_{cd}(0) \rangle_{R \times S^3}. \quad (4.10)$$

We are interested in calculating correlation functions of local gauge invariant single trace operators. In the AdS-CFT correspondence, these correlation functions correspond to closed string amplitudes. In terms of the propagator on $R \times S^3$, each propagator, which corresponds to an edge of a 't Hooft-Feynman diagram, has sum over images appearing in the righthand side of (4.10). This sum in the 't Hooft-Feynman diagram can be reorganized into the sum over index loops, interaction vertices and cycles on handles through the relation

$$E = F + V - (2 - 2g) = (F - 1) + (V - 1) + 2g. \quad (4.11)$$

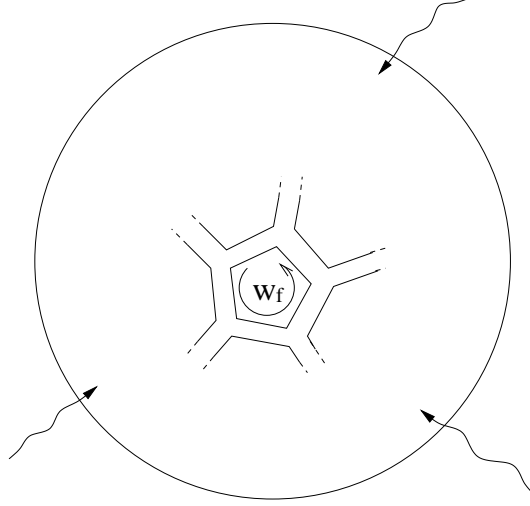


Figure 6: The winding number w_f is associated with the f -th index loop, or the face of the simplicial decomposition.

This can be interpreted as sum over $F-1$ loops of the Feynman diagram, $V-1$ independent positions of the images of the interaction vertices (only the relative positions matter), and two cycles associated with each handle. Then for a given Feynman diagram, we have the following overall factor from the index loops:

$$\langle \text{tr}U^{w_1} \text{tr}U^{w_2} \dots \text{tr}U^{w_{F-1}} \rangle_{A_0} \quad (4.12)$$

where

$$\langle F(A_0) \rangle_{A_0} \equiv \int dA_0 F(A_0) e^{-S_{eff}(A_0)}. \quad (4.13)$$

Here w_f is the winding number associated with the f -th loop (Fig.6):

$$w_f \equiv \sum_{\text{Edges on } f\text{-th loop}} n_l, \quad (4.14)$$

where n_l is the number associated with the l -th edge(=propagator) which is on the f -th loop, labeling the images in the righthand side of (4.10). w_f counts how many times the f -th index loop wind around the thermal circle. From (4.12), we observe that *the expectation value of the Polyakov loop winding w times around the thermal circle, introduced in (3.4), gives the weight to the w time-winding of a loop in the Feynman diagrams.* Note that this is nothing but the w -th Fourier mode of the eigen-states density $\rho(\theta)$, (3.21) in section 3.²⁰

²⁰We thank T. Matsuo and S. Wadia for discussions on this point.

So far, we were discussing $1/N$ expansion but hasn't taken the $N \rightarrow \infty$ limit. The eq.(4.12) is applicable for finite N [43]. Now, let us consider the $N \rightarrow \infty$ planer limit. Then, in the confined phase all the expectation value of the Polyakov loops vanish and only diagrams with zero-winding numbers on their index loops contribute. This means that one needs to sum over images only for the interaction vertices and the external single trace operators. However, the path integration over the position on S^1 together with the sum over images recovers the path integral over entire R because

$$\sum_{n=-\infty}^{\infty} \int_0^{\beta} d\tau f(\tau + n\beta) = \int_{-\infty}^{\infty} d\tau f(\tau) \quad (4.15)$$

for any function f . That means, *the path integral for the internal loops is the same as that of the uncompactified theory*, the theory on $R \times S^3$. Thus in terms of the correlation functions on $R \times S^3$, the correlation functions on $S^1 \times S^3$ in the confined phase is expressed as

$$\begin{aligned} & \langle \mathcal{O}_1(\tau_1) \mathcal{O}_2(\tau_2) \cdots \mathcal{O}_n(\tau_n) \rangle_{S^1 \times S^3} \\ &= \sum_{m_1, \dots, m_{n-1} = -\infty}^{\infty} \langle \mathcal{O}_1(\tau_1 + m_1\beta) \mathcal{O}_2(\tau_2 + m_2\beta) \cdots \mathcal{O}_n(\tau_n) \rangle_{R \times S^3}, \end{aligned} \quad (4.16)$$

where \mathcal{O}_i 's are local gauge invariant single trace operators. As we have mentioned above, there are sum over images for the external operators but one. Note that for composite operators \mathcal{O}_i , (4.16) is *not* a straightforward consequence that the time direction is compactified, but the winding modes associated with the index loops must be suppressed. As we have seen, the essential reason for this suppression was that we were in the confined phase. This mechanism that the result of the compactified theory can be obtained from the un-compactified theory (or vice versa), or in other words the correlation functions do not essentially depend on the radius of the compactification radius, is known as the large N reduction [44]. Its role in the context of AdS-CFT was first noticed in [14] and was further investigated in [45] (see also [43]). In the bulk side, this means that the geometry corresponding to the confined phase is the simple periodic identification of the geometry of the zero-temperature theory, i.e. AdS_5 for the $\mathcal{N} = 4$ super Yang-Mills theory: If one identifies \mathcal{O}_i with the closed string field in the bulk, (4.16) is nothing but the method of images *in the bulk*. (How to read off the bulk geometry from the gauge theory 't Hooft-Feynman diagrams is far from being completely understood, much remains to be investigated. However, see [7, 8] for suggestive examples of how at zero-temperature the bulk geometry seems to emerge from the gauge theory 't Hooft-Feynman diagrams.) In section 2 we obtained the same result in the gravity side, which correspond to the strong

't Hooft coupling region. Here, instead, we started from the perturbative Yang-Mills side and read off the geometry.

In the deconfined phase, the expectation value of the Polyakov loops has vacuum expectation value and from (4.12) we observe that the winding modes associated with the index loops contribute. This statement is valid for finite N . In the $N \rightarrow \infty$ limit, we can apply the saddle point approximation, for example, as we have seen in section 3. In the simple toy model there, the deconfinement transition temperature was the point where the first Fourier mode of the eigen-value density, or the winding number one Polyakov loop, becomes unstable See eq.(3.20) and the explanations there. In order to obtain closed string worldsheets from the 't Hooft-Feynman diagrams, one must somehow “glue” the face of the 't Hooft-Feynman diagrams.²¹ However, the non-zero winding number on a face is an obstruction for such glueing. This makes closed string interpretation difficult in the (trivial periodic identification of the) zero-temperature bulk geometry. From the closed string point of view, these winding modes associated with the index loops corresponds to vortices on the worldsheet.²² Therefore, we have seen that the deconfinement corresponds to the vortex condensation on the worldsheet.²³ Notice that the above explanation is based on the use of the propagator on $R \times S^3$, i.e. the righthand side of (4.10). In the bulk, this corresponds to the expansion around (a simple periodic identification of) the zero-temperature geometry. If we want a closed string worldsheet interpretation, this is not an appropriate background in the deconfined phase. The target space geometry must be deformed by the vortex/winding mode condensation on the worldsheet. The geometry after the vortex/winding mode condensation should be probed by using the expression of the propagator in the lefthand side of (4.10) (i.e. the form *after* summed over). Since there is no sum over images in the lefthand side of (4.10), this should correspond to the bulk geometry without a non-contractible circle, see Fig.2. And since there's no winding

²¹See [8, 9] for a proposal for the precise prescriptions for this glueing.

²²The worldsheet theory should have a coordinate field $\tau(\sigma^0, \sigma^1)$ corresponding to the τ direction in the target space, where σ 's are worldsheet coordinates. The winding in the target space τ direction means $\tau(\sigma^0, \sigma^1 + 2\pi) = \tau(\sigma^0, \sigma^1) + \omega\beta$, where ω is the winding number. Let us change the worldsheet coordinates to $z = \exp(\sigma^0 + i\sigma^1)$. Then, ω is the winding number counting how many times the field $\tau(z)$ wrap around the target space circle as we go around $z = 0$: $z \rightarrow ze^{2\pi i}$. Such configuration is called vortex with vorticity ω . $\tau(z)$ should corresponds to the τ coordinate of a point on the random surface given by the 't Hooft-Feynman diagram.

²³This type of phase transitions in two dimensions caused by the vortex condensation are called Berezinsky-Kosterlitz-Thouless transition [46, 47, 48]. See for example the insightful book [49] for explanations, from which the contents of [46] can partially be known.

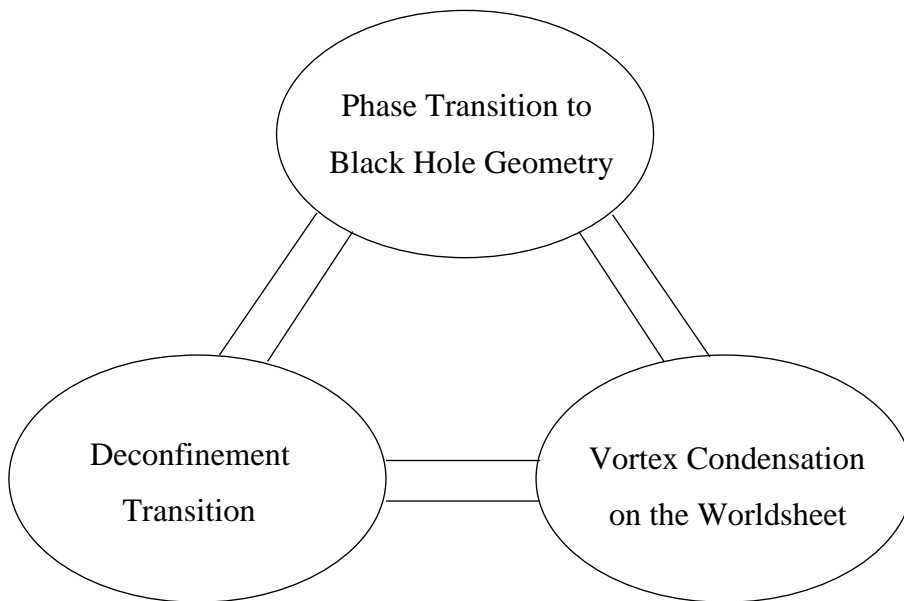


Figure 7: The suggested equivalence of the three phase transitions.

mode if we use the lefthand side of (4.10), it should in principle be possible to “glue” the faces of the ’t Hooft-Feynman diagram.²⁴ Thus in the ’t Hooft-Feynman diagrams, the difference of the bulk topology corresponds to whether or not it is appropriate to use the propagator on $S^1 \times S^3$ (lefthand side of (4.10)) or the propagator on $R \times S^3$ (righthand side of (4.10)). Hence the ’t Hooft-Feynman diagrams at least can probe the difference of the topology of the bulk geometry. Compare the expectation from the gravity/string side in section 2.

Thus, from the analysis of the ’t Hooft-Feynman diagrams at finite temperature, we arrived at the picture that *the Hawking-Page transition to the black hole geometry, the deconfinement transition in gauge theories, and the vortex condensation on the closed string worldsheets are all equivalent* (Fig.7). This is the first main message of this lecture note. Of course, this equivalence should be made more precise by making the AdS-CFT conjecture more concrete.

It has been expected that the Hagedorn transition in string theory indicates the appearance of more fundamental degrees of freedom, like the deconfinement transition in the gauge theory [50]. The origin of the Hagedorn transition was identified with the vortex condensation on string worldsheets in [51, 52]. It is intriguing that the above picture

²⁴Although we do not yet have a prescription for glueing as precise as that in the zero temperature case of [8, 9] in this case.

we have arrived tells that the Hagedorn transition *is* the deconfinement transition, the equivalence being given via the AdS-CFT duality. From this point of view, it is quite curious that we still seem to have closed string description even after the deconfinement, although gauge non-singlet states which are not identified as close string excitations also begin to play a role.

It may be worthwhile to point out that the order of the phase transition is model dependant. But the analysis of the 't Hooft-Feynman diagram does not get modified much. This is because the phase is determined by the effective action of the eigenvalues studied in the previous section, and the 't Hooft-Feynman diagrams just probe it. Most Yang-Mills theories on S^3 at weak coupling seem to give rise to the first order deconfinement phase transition [5, 6]. That means the phase transition generically could occur before the tachyonic mode appears. But whatever the order of the phase transition is, the deconfined phase corresponds to the vortex-condensate phase on the worldsheet.

The analysis of the 't Hooft-Feynman diagrams in this section is closely related to those in [53, 54, 55] studied in the context of a matrix model for the two-dimensional black hole. (See [56, 57, 58] for earlier studies on vortex condensation in matrix models.) If we regard the AdS-CFT correspondence as a particular example of more general open-closed string duality, our AdS₅-CFT₄ model and the two-dimensional model may be looked from a unified view.²⁵ The analysis of the 't Hooft-Feynman diagram in AdS-CFT at finite temperature was studied in [14] in the context of the Gopakumar's program [7, 8, 9, 10, 11, 12]. See also [60, 43] for related discussions. Some explanations in this section follow the reference [43]. Although there is an advantage in seeing the two-dimensional model and AdS-CFT from the unified view-point, one should also be aware of some technical differences. In the AdS₅-CFT₄ case, the effective action exhibits phase transition by just varying the temperature, whereas in the two-dimensional model one needs to deform the matrix model itself by adding a potential for the eigen-values of the gauge field (change of the measure $[d\Omega] \rightarrow [d\Omega]_\lambda$ in [53]), in order to obtain the deconfined phase which should correspond to the black hole geometry.²⁶ Recall that in section 3 we needed $d \geq 2$ to have phase transition at finite transition temperature. This indicates it is not straightforward to obtain S_{eff} which exhibits the deconfinement transition at

²⁵This view was already there in [53]. That the matrix model for the two-dimensional black hole can be practically analyzed in the way parallel to the AdS-CFT case was stressed in [59], where the expectation value of the Polyakov loop was calculated both from the matrix model and from the closed string theory.

²⁶In the case of AdS₅-CFT₄, the change of the temperature in the same theory changes the effective matrix model of A_0 .

finite temperature by integrating out a field in matrix models for two-dimensional target space. Also at this moment the holography seems to be best understood in asymptotically AdS spaces. On the otherhand, the closed string worldsheet theory seems to be better understood in the two-dimensional model [53, 61]. Finally, we may encounter more qualitative differences between open-closed duality based on stable D-branes (AdS₅ case) and unstable D-branes (matrix models for two-dimensional strings) if we go into more detailed examinations.

The analysis of the previous section and this section clearly shows that it is of essential importance, particularly at finite temperature, that the world-volume theory on D-branes is not just a matrix field theory but a gauge theory. This point was not appreciated much in the old studies of the matrix models, but began to be realized after [62].

5 't Hooft-Feynman Diagrams at Finite Temperature – Real Time Formalism

5.1 Motivation

In the previous sections, we have studied thermodynamics in the Euclidean time formalism (the imaginary time formalism). As we have seen in section 2, the Euclidean geometry only covers the region outside the black hole horizon. However, the real problems about black holes, such as the information loss paradox and curvature singularities, arise from inside the black hole. Hence it is important to develop a method which can treat the Lorentzian time signature case. In the boundary field theory side, this should correspond to a field theory at finite temperature in the Lorentzian signature. The formulation of a field theory at finite temperature with the Lorentzian time signature is generally called the real time formalism. We will explain two such formalisms below: One is the thermo-field dynamics and the other is the closed-time-path formalism.

In the real time formulation of finite temperature field theories [63, 64, 65, 66],²⁷ it seems almost necessary to introduce an additional set of fields besides the original ones (those in the zero-temperature theory). Each of the newly introduced field is associated with a field in the original theory. (In this note we will refer to the newly introduced fields as type-2 fields, as opposed to the original fields which we will call type-1 fields.) On the

²⁷For further learning of the real time formulation of field theories at finite temperature, see e.g. [67, 68] for general aspects, [69] for insightful exploration of the thermo-field dynamics, [70] for BRS quantization of gauge theories.

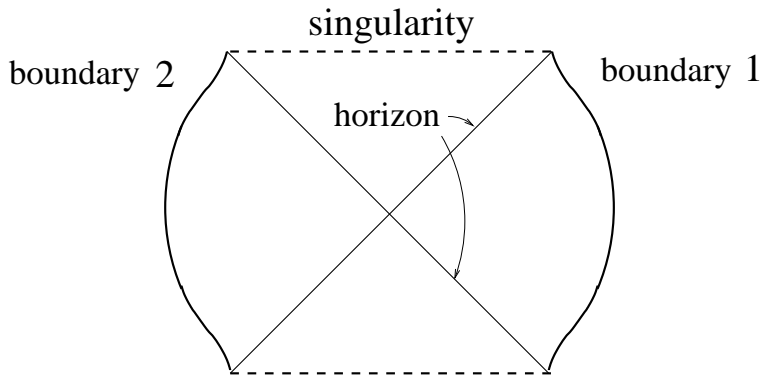


Figure 8: The Carter-Penrose diagram of the maximally extended AdS-Schwarzschild black hole geometry. Spherical directions are suppressed in the figure. Besides the usual boundary of the AdS space at spatial infinity (boundary 1, see also Fig.9), there is a second boundary behind the horizon (boundary 2). For more detail, see e.g. [71].

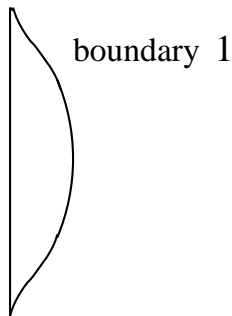


Figure 9: The Carter-Penrose diagram of the AdS geometry.

other hand, the Carter-Penrose diagram of the maximally extended AdS-Schwarzschild black hole geometry has a boundary behind the horizon (Fig.8 boundary 2), in addition to the usual boundary of the AdS space at spatial infinity outside the horizon (Fig.8 boundary 1). In the context of the AdS-CFT correspondence, the type-2 fields in the boundary CFT was identified as the degrees of freedom behind the black hole horizon [72, 73, 74].²⁸ This gives a nice explanation for the necessity of the introduction of type-2 fields in the real time formulation of the finite temperature field theory.

However, as we have seen in section 2, below the Hawking-Page transition temperature the thermodynamically preferred configuration in canonical ensemble is the thermal AdS without a black hole. Since it is a finite temperature system, the dual gauge theory should

²⁸See also [75] for an approach to describe the path integral formulation of the real time formalism from the gravity side in black hole phase.

still be described by the real time formulation for the finite temperature. Thus one must conclude that below the Hawking-Page transition temperature, the type-2 fields in the dual gauge theory cannot correspond to the degrees of freedom behind the black hole horizon, since there is no black hole at all. But then, what is the dual bulk description for the type-2 fields in this case? Since the AdS geometry corresponds to the confined phase in gauge theory side, the confinement should change the role of the type-2 fields in the bulk. We will show that this is indeed the case: In the confined phase, the role of type-2 fields in the gauge theory is to make up *bulk* type-2 fields of closed string field theory on AdS at finite temperature in the real time formalism. In this section, we will explain how this is described from the Yang-Mills theory. Since the bulk is also at finite temperature, it is natural that the bulk theory also has the type-2 fields of its own. The discussions will be in the leading order in the $1/N$ expansion, which corresponds to the classical theory in the bulk. Since the Carter-Penrose diagram is based on classical gravity, this is sufficient for explaining why we should not obtain the region behind the horizon in this case.

5.2 Thermo-field dynamics

The quantities we are interested in field theories at finite temperature are expectation values of operators in the canonical ensemble:

$$\text{Tr} \left\{ e^{-\beta \hat{H}} \mathcal{O}_1(t_1) \mathcal{O}_2(t_2) \cdots \mathcal{O}_n(t_n) \right\}. \quad (5.1)$$

Since the Hisenberg operators $\mathcal{O}_i(t_i)$ depend on time, the imaginary time formalism is not applicable.²⁹ Thermo-Field Dynamics (TFD) [63] is a formalism in which (5.1) is calculated as a kind of “vacuum” expectation value. For that purpose, one first double the Hilbert space by preparing a copy of the original one. We will label the original operators and states with suffix 1, and their copies with suffix 2. Then we introduce “thermal vacuum” at inverse temperature β by

$$|0, \beta\rangle \equiv \sum_n e^{-\frac{\beta E_n}{2}} |E_n\rangle_1 |E_n\rangle_2, \quad (5.2)$$

where $|E_n\rangle$ is the energy eigen-state with the eigenvalue E_n . The thermal vacuum is invariant under time translation with respect to the Hamiltonian H_{TFD} defined by

$$\hat{H}_{TFD} = \hat{H}_1 - \hat{H}_2, \quad (5.3)$$

²⁹The relation between the real time correlation functions and those analytically continued from the imaginary time formalism are not simple in general. See e.g. [76].

where \hat{H}_1 is the original Hamiltonian, and \hat{H}_2 is the copy acting on the copy Hilbert space. It is easy to see that by the use of the thermal vacuum, (5.1) can be written in the form of a vacuum expectation value:

$$\langle 0, \beta | \mathcal{O}_1 \cdots | 0, \beta \rangle = \sum_n e^{-\beta E_n} \langle E_n | \mathcal{O}_1 \cdots | E_n \rangle_1 = \text{Tr}_1 \{ e^{-\beta \hat{H}_1} \mathcal{O}_1 \cdots \}. \quad (5.4)$$

In the above operators are all original ones which we have given the suffix 1. Now let us consider applying this formalism to the large N gauge theories, in the context of the AdS-CFT correspondence. In the confined phase, the energy eigen-states are given by gauge singlets. If we identify those states constructed by acting local gauge invariant single trace operators on the vacuum with states in the closed string theory following the standard AdS-CFT dictionary (see [77]), we should obtain the thermo-field dynamics for the closed string field theory. As long as we are using the same energy eigen-states as those of zero-temperature case, we should also obtain the same bulk geometry on a time-slice. However, in this explanation it is not obvious whether it is appropriate to keep on using the zero-temperature energy eigen-states, i.e. why corrections by the effect of the temperature can be neglected. In the bulk, this corresponds to whether we obtain the AdS geometry as an appropriate background or not at finite temperature. This question is basically solved by the large N reduction explained in the previous section. But we should look for the real time version of the large N reduction.

We will investigate this using the path integral formulation of the gauge theory at finite temperature in the real time formalism. Since the covariant path integral approach was the most efficient way to calculate closed string amplitudes in critical string theories, it would also be useful to investigate this method in our case. This also allows us to see how the expectation value of Polyakov loops we studied in section 3 are reflected on the closed string worldsheets.

We will mainly describe the confined phase case below, but the difference from the deconfined phase will be mentioned. Our ultimate objective will be to understand how black holes are described in the dual Yang-Mills theory. But in order to understand the black hole, it is important to understand first how the situation without a black hole is described in Yang-Mills theory. Once this is understood, then we can study the difference between that and the Yang-Mills description of the black hole geometry.

5.3 Path integral method in the real time formalism

In this section, we will review the path integral method in the real time formulation of finite temperature field theories [66]. This path integral formulation of field theory at finite temperature in the real time can be regarded as a special case of the Schwinger-Keldysh closed-time-path formalism [78, 79] which was formulated with an attempt to describe non-equilibrium systems. We would like to apply this formalism to the large N gauge theories. A concrete example in mind is the $\mathcal{N} = 4$ super Yang-Mills theory with $SU(N)$ gauge group on S^3 in the 't Hooft limit, but we will consider a simpler model which captures the essential point. We take a real scalar field $\Phi_{ab}(t)$ in the adjoint representation of $SU(N)$ as an example. Here, a, b are $SU(N)$ gauge indices. It is straightforward to include several scalar fields, fermions or dynamical gauge fields. Since the dependence on the spatial S^3 direction is not essential in the following argument, we can first consider a quantum mechanical model obtained from the dimensional reduction. It is easy to incorporate the dependence on the S^3 directions.

The quantities we will be interested are thermal Green's functions $G_\beta(t_1, \dots, t_n)$ of the time-ordered products of operators $\hat{\Phi}(t)$ in Heisenberg picture:

$$G_\beta(t_1, \dots, t_n) = \frac{1}{\text{Tr} e^{-\beta \hat{H}}} \text{Tr} \left\{ e^{-\beta \hat{H}} T[\hat{\Phi}(t_1) \cdots \hat{\Phi}(t_n)] \right\}, \quad (5.5)$$

where “Tr” is the trace over *physical* states satisfying the Gauss' law constraints:

$$\hat{\rho}_{ab} |phys\rangle = 0. \quad (5.6)$$

Here $\hat{\rho}_{ab} = i : ([\hat{\Phi}, \hat{\Pi}_\Phi])_{ab} :$ is the generator of the gauge transformation, where $\hat{\Pi}_{\Phi ab}$ is the conjugate momentum of $\hat{\Phi}_{ab}$ and $: : :$ denotes the normal ordering. $T[\cdots]$ above denotes the time ordering and β is the inverse temperature. We will study the Hamiltonian \hat{H} given by

$$\hat{H} = \text{tr} \left\{ \frac{g^2}{2} \hat{\Pi}_\Phi \hat{\Pi}_\Phi + \frac{\omega^2}{2g^2} \hat{\Phi}^2 + \frac{1}{g^2} V[\hat{\Phi}] \right\}, \quad (5.7)$$

where g is the gauge coupling constant, “tr” is a trace over the $SU(N)$ gauge group indices and $V[\hat{\Phi}]$ is a potential term. The mass ω is proportional to the inverse radius of S^3 in the case when the quantum mechanics is obtained from the compactification of four dimensional conformal field theory on S^3 . In order to evaluate the thermal Green's functions by the path integral method, we should extend the support of the field variables to the whole complex t -plane:

$$\hat{\Phi}(t) = e^{i\hat{H}t} \hat{\Phi}(0) e^{-i\hat{H}t}. \quad (5.8)$$

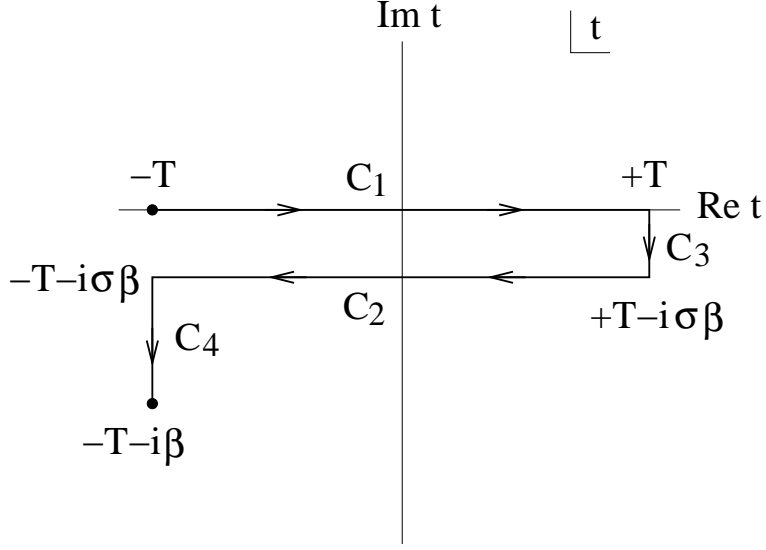


Figure 10: The contour C

We would like to obtain a functional representation for the generating functional $Z[J]$ such that:

$$G_\beta(t_1, \dots, t_n) = \frac{1}{Z(0)} \frac{1}{i^n} \frac{\delta}{\delta J(t_n)} \cdots \frac{\delta}{\delta J(t_1)} Z[J] \Big|_{J=0}. \quad (5.9)$$

The functional

$$\text{Tr} \left\{ e^{-\beta \hat{H}} T \left[e^{i \int_{-T}^T dt J(t) \hat{\Phi}(t)} \right] \right\} \quad (5.10)$$

has this property when $-T < t_i < T$. But in order to calculate the thermal Green's function perturbatively, we should extend the t integration to a contour C on the complex plane:

$$Z[J] = \text{Tr} \left\{ e^{-\beta \hat{H}} T_C \left[e^{i \int_C dt J(t) \hat{\Phi}(t)} \right] \right\} \quad (5.11)$$

where the contour C is depicted in Fig.10.³⁰ $T_C[\dots]$ denotes time-ordering along the contour C . We insert the identity $1 = e^{-i\hat{H}T} e^{i\hat{H}T}$ and then use the cyclic property of the trace. We can also regard $e^{-\beta \hat{H}}$ as a time translation in the imaginary direction. Then (5.11) can be rewritten as

$$\int d\Phi \int d\Phi' \int d\Phi'' \int d\Phi'''$$

³⁰There is some arbitrariness in the choice of the contour. It should be everywhere non-increasing in the imaginary direction in order for the expression to be convergent in the $T \rightarrow \infty$ limit.

$$\langle \Phi, -T | T_{C_1} [e^{i \int_{C_1} dt J(t) \hat{\Phi}(t)}] | \Phi', T \rangle \quad (5.12)$$

$$\langle \Phi', T | T_{C_3} [e^{i \int_{C_3} dt J(t) \hat{\Phi}(t)}] | \Phi'', T - i\sigma\beta \rangle \quad (5.13)$$

$$\langle \Phi'', T - i\sigma\beta | T_{C_2} [e^{i \int_{C_2} dt J(t) \hat{\Phi}(t)}] | \Phi''', -T - i\sigma\beta \rangle \quad (5.14)$$

$$\langle \Phi''', -T - i\sigma\beta | T_{C_4} [e^{i \int_{C_4} dt J(t) \hat{\Phi}(t)}] | \Phi, -T - i\beta \rangle \quad (5.15)$$

where $|\hat{\Phi}, z\rangle$ is the eigen-state of the Heisenberg operators:

$$\hat{\Phi}(z)|\Phi, z\rangle = \Phi|\Phi, z\rangle, \quad |\Phi, z\rangle = e^{i\hat{H}z}|\Phi\rangle, \quad (5.16)$$

and z can be a complex number. We have matched the eigen-states of the Heisenberg operators with the eigen-states of the Schrödinger operators at $z = 0$. The projections to the physical states (5.6) is understood in the above expression. When $\sigma = \frac{1}{2}$, the time evolution on the vertical part of the contour (5.14) is essentially equivalent to preparing the thermal vacuum (5.2) of the thermo-field dynamics. (We will take $T \rightarrow \infty$ and $J(t) \rightarrow 0$ as $t \rightarrow \pm\infty$. To see the above, one just needs to change the notation: One changes “ket” of the matrix elements of (5.13) to “bra”, and regard them as states in doubled Hilbert space. Then the matrix elements of (5.12) and (5.14) are combined into matrix elements acting on this doubled Hilbert space. Similar for the matrix elements of (5.15).) By further inserting a complete set of physical states satisfying (5.6), we obtain the path integral representation of the generating functional $Z[J]$:

$$Z[J] = \int [\mathcal{D}_C \Phi] e^{i \int_C dt \{\mathcal{L}[\Phi] + J(t)\Phi(t)\}}, \quad (5.17)$$

where $\mathcal{L}[\Phi]$ is the Lagrangian

$$\mathcal{L}[\Phi] = \frac{1}{g^2} \text{tr} \left\{ \frac{1}{2} D_t \Phi D_t \Phi - \frac{\omega^2}{2} \Phi^2 - V[\Phi] \right\}. \quad (5.18)$$

The covariant derivative is given by

$$(D_t \Phi)_{ab} = \partial_t \Phi_{ab} - i[A_0, \Phi]_{ab}, \quad (5.19)$$

and the gauge field A_0 has been introduced while imposing the Gauss' law constraints as delta function. The path integral is over the fields which satisfy the boundary conditions

$$\Phi_{ab}(-T - i\beta) = \Phi_{ab}(-T), \quad (5.20)$$

following from the trace over the Hilbert space in (5.5). We can rewrite (5.17) as

$$Z[J] = \exp \left\{ -i \int_C dt V \left[\frac{1}{i} \frac{\delta}{\delta J} \right] \right\} \exp \left\{ -\frac{i}{2} g^2 \int_C dt \int_C dt' J_{ab}(t) D_{ab,cd}^C(t-t') J_{cd}(t') \right\}, \quad (5.21)$$

where the thermal propagator $D_{ab,cd}^C(t-t')$ is a Green's function on the contour

$$(-\partial_t^2 - \omega^2)D_{ab,cd}^C(t-t') = \delta_C(t-t')\delta_{ad}\delta_{bc}, \quad (5.22)$$

subject to the boundary condition following from (5.20). Here $\delta_C(t-t')$ is the delta function defined on the contour:

$$\int_C dt \delta_C(t-t') f(t) = f(t'). \quad (5.23)$$

The boundary of the time T is eventually taken to infinity. By taking $J(t) \rightarrow 0$ as $t \rightarrow \pm\infty$, the generating functional factorizes as

$$Z[J] = Z_{12}[J]Z_{34}[J], \quad (5.24)$$

where $Z_{12}[J]$ (respectively $Z_{34}[J]$) denotes the contribution from the path C_1 and C_2 (C_3 and C_4). The effect of finite temperature enters in the propagators through the boundary condition (5.20). Although the generating functional can be seen to factorize, $Z_{34}[J]$ part plays a role for modifying the boundary conditions on the Green's function, as we will see below.

5.4 Incorporating the effect of the confined phase background

In this subsection we present a prescription for reading off the dual bulk description corresponding to the confined phase in the real time formalism. When there are no external operator insertions, one can take the Matsubara contour, i.e. the line straight down from $-T$ to $-T - i\beta$. Then the calculation reduces to that in the imaginary time formalism. As we have seen in section 3, the confined phase is characterized by the vanishing of the expectation value of the Polyakov loop. The large N saddle point value of the temporal gauge field A_0 was given by

$$\frac{\partial}{\partial \tau} A_{0ab} = 0, \quad A_{0ab} = \delta_{ab} \frac{2\pi}{\beta N} \left(a - \frac{N+1}{2} \right), \quad (5.25)$$

in an appropriate gauge. (5.25) corresponds to the constant eigen-value density $\rho(\theta) = \frac{1}{2\pi}$ in the large N limit (see section 3). This gives an appropriate expansion point for perturbative calculation on the vertical parts of the contour.

As we have seen in the previous section, in the imaginary time formalism it was essential to expand around the saddle point of A_0 (5.25) to read off the dual bulk geometry in the confined phase. Therefore, also in the real time formalism, the correct prescription for reading off the dual bulk description corresponding to the confined phase should be to

include the saddle point value (5.25) of A_0 into the Green's function *on the vertical parts of the contour*. Thus, instead of (5.22), we use Green's function which satisfies

$$(-D_t^2 - \omega^2)D_{ab,cd}^C(t-t') = \delta_C(t-t')\delta_{ad}\delta_{bc} \quad , \quad (5.26)$$

where on the vertical parts of the contour we have included the saddle point value of A_0 (5.25) in the covariant derivative D_t . On the horizontal parts of the contour one can choose $A_0 = 0$ gauge. Since we are including the effect of the A_0 configuration (5.25) on the vertical parts of the contour, it is convenient to define the field

$$\tilde{\Phi}_{ab}(t) = e^{-2\pi i \frac{a-b}{\beta N} (\text{Im} t)} \Phi_{ab}(t) \quad (5.27)$$

so that the differential equation for the Green's function $\tilde{D}^C(t-t')$ for $\tilde{\Phi}(t)$ takes the form of the ordinary one (5.22):

$$(-\partial_t^2 - \omega^2)\tilde{D}_{ab,cd}^C(t-t') = \delta_C(t-t')\delta_{ad}\delta_{bc} \quad . \quad (5.28)$$

However, the field redefinition (5.27) modifies the boundary condition (5.20) to

$$\tilde{\Phi}_{ab}(-T - i\beta) = e^{2\pi i \frac{a-b}{N}} \tilde{\Phi}_{ab}(-T). \quad (5.29)$$

One can solve (5.22) with the ansatz

$$\tilde{D}_{ab,cd}^C(t-t') = \theta_C(t-t')\tilde{D}_{ab,cd}^>(t-t') + \theta_C(t'-t)\tilde{D}_{ab,cd}^<(t-t'), \quad (5.30)$$

where $\theta_C(t-t')$ is the step function defined on the contour:

$$\theta_C(t-t') = \int_C dt'' \delta_C(t''-t'). \quad (5.31)$$

Since from (5.17) to (5.21) the change of variable

$$\tilde{\Phi}_{ab}(t) \rightarrow \tilde{\Phi}_{ab}(t) + \int_C dt' \tilde{D}_{ab,cd}(t-t') J_{cd}(t'), \quad (5.32)$$

has been made, the boundary condition (5.29) implies

$$\tilde{D}_{ab,cd}^>(t-t'-i\beta) = e^{2\pi i \frac{a-b}{N}} \tilde{D}_{ab,cd}^<(t-t'). \quad (5.33)$$

The unique solution to (5.28) with the boundary condition (5.33) is

$$\tilde{D}^C(t-t')_{ab,cd} = \frac{-i}{2\omega} \left[(Ae^{-i\omega t} + Be^{i\omega t})\theta_C(t-t') + (Ce^{-i\omega t} + De^{i\omega t})\theta_C(t'-t) \right] \quad (5.34)$$

with

$$\begin{aligned} A &= \frac{1}{1 - e^{-\beta\omega - 2\pi i \frac{a-b}{N}}}, & B &= \frac{e^{-\beta\omega + 2\pi i \frac{a-b}{N}}}{1 - e^{-\beta\omega + 2\pi i \frac{a-b}{N}}}, \\ C &= \frac{e^{-\beta\omega - 2\pi i \frac{a-b}{N}}}{1 - e^{-\beta\omega - 2\pi i \frac{a-b}{N}}}, & D &= \frac{1}{1 - e^{-\beta\omega + 2\pi i \frac{a-b}{N}}}. \end{aligned} \quad (5.35)$$

The Green's function (5.34) can be rewritten in the spectral representation:

$$i\tilde{D}_{ab,cd}^C(t-t') = \int_{-\infty}^{\infty} \frac{dk_0}{2\pi} e^{-ik_0(t-t')} \rho(k_0) [\theta_C(t-t') + N(k_0, a-b)] \delta_{ad} \delta_{bc}, \quad (5.36)$$

where

$$\rho(k_0) = 2\pi \varepsilon(k_0) \delta(k_0^2 - \omega^2), \quad \varepsilon(k_0) = \theta(k_0) - \theta(-k_0) \quad (5.37)$$

and

$$N(k_0, a-b) = \frac{1}{e^{\beta k_0 + 2\pi i \frac{a-b}{N}} - 1}. \quad (5.38)$$

As in (5.24), the partition function factorizes. Therefore, only the propagators between the fields on the contours C_1 or C_2 need to be considered. The propagators for general σ ($0 < \sigma < 1$, where σ is given in Fig.10) are obtained as

$$\tilde{D}_{ab,cd}^{(11)}(t-t') = \tilde{D}_{ab,cd}^C(t-t'), \quad (5.39)$$

$$\tilde{D}_{ab,cd}^{(22)}(t-t') = \tilde{D}_{ab,cd}^C((t - i\sigma\beta) - (t' - i\sigma\beta)), \quad (5.40)$$

$$\tilde{D}_{ab,cd}^{(12)}(t-t') = \tilde{D}_{ab,cd}^<(t - (t' - i\sigma\beta)), \quad (5.41)$$

$$\tilde{D}_{ab,cd}^{(21)}(t-t') = \tilde{D}_{ab,cd}^>((t - i\sigma\beta) - t'). \quad (5.42)$$

Notice that the propagator takes the form of a 2×2 matrix. This can be looked as the degrees of freedom are doubled compared with the original theory at zero temperature. The doubling of the degrees of freedom originates from the two parts of the contour C_1 and C_2 in Fig.10. $\tilde{D}^{(11)}$ (respectively $\tilde{D}^{(22)}$) is regarded as a propagator between type-1 (type-2) fields, and $\tilde{D}^{(12)}$ and $\tilde{D}^{(21)}$ are mixed propagators between type-1 and type-2 fields.

By taking $\sigma = \frac{1}{2}$ we obtain the most symmetric expression. It is convenient to split the propagator into a temperature dependent part and an independent part. Also, at this point it is convenient to undo the field redefinition (5.27) to obtain a symmetric expression for the propagators. In momentum space, they are given by

$$iD_{ab,cd}^{(rs)} = iD_{0ab,cd}^{(rs)} + iD_{\beta ab,cd}^{(rs)} \quad (r, s = 1, 2), \quad (5.43)$$

$$iD_{0ab,cd} = \delta_{ad}\delta_{bc} \begin{pmatrix} \frac{i}{k_0^2 - \omega^2 + i\epsilon} & 0 \\ 0 & \frac{-i}{k_0^2 - \omega^2 - i\epsilon} \end{pmatrix}, \quad (5.44)$$

$$iD_{\beta ab,cd} = \delta_{ad}\delta_{bc}\pi\delta(k_0^2 - \omega^2) \times \frac{1}{e^{|\beta k_0 + 2\pi i \frac{a-b}{N}|_R} - 1} \begin{pmatrix} 1 & e^{\frac{1}{2}|\beta k_0 + 2\pi i \frac{a-b}{N}|_R} \\ e^{\frac{1}{2}|\beta k_0 + 2\pi i \frac{a-b}{N}|_R} & 1 \end{pmatrix}. \quad (5.45)$$

In the above, $|\cdots|_R$ is defined as

$$|z|_R = \begin{cases} z & (\text{Re } z > 0) \\ -z & (\text{Re } z < 0) \end{cases}, \quad (\text{Re } z \neq 0). \quad (5.46)$$

Eq.(5.46) is not defined for $\text{Re } z = 0$, but because of the on-shell delta function in (5.45) one does not need to consider that case as long as $\omega \neq 0$. Notice the gauge index dependant phases in (5.45) which arouse from our prescription for incorporating the effect of the confined phase background. These will play the crucial roles in the following discussions.

Perturbative Feynman rules can be obtained just as in the conventional field theories and are sketched in Fig.11. (1) represents the temperature independent part of the propagator $iD_{0ab,cd}^{(rs)}$ and (2) the temperature dependent part $iD_{\beta ab,cd}^{(rs)}$. The temperature dependent part of the propagator is drawn with the “cut” line in Fig.11 (2). This cut is one of the most important tools we will use repeatedly in the following discussions. Type-1 fields and type-2 fields are coupled only through the propagators: The interaction vertices do not mix type-1 and type-2 fields. The interaction vertices of type-2 fields ($\times i$) are given by the complex conjugate of those of type-1 fields:

$$i \text{tr} V_2[\Phi_{(2)}] = (i \text{tr} V_1[\Phi_{(1)}])^* \Big|_{\Phi_{(1)} \rightarrow \Phi_{(2)}}. \quad (5.47)$$

We have assumed that the potential is real.

5.5 The vanishing mechanism and surviving diagrams as real time closed string diagrams

In this subsection, with the prescription for incorporating the effect of the confined phase background (5.25) discussed in the previous subsection, we will show that the contributions from a large class of Feynman diagrams vanish. The quantities of our interest are the correlation functions of gauge invariant single trace local operators, which correspond

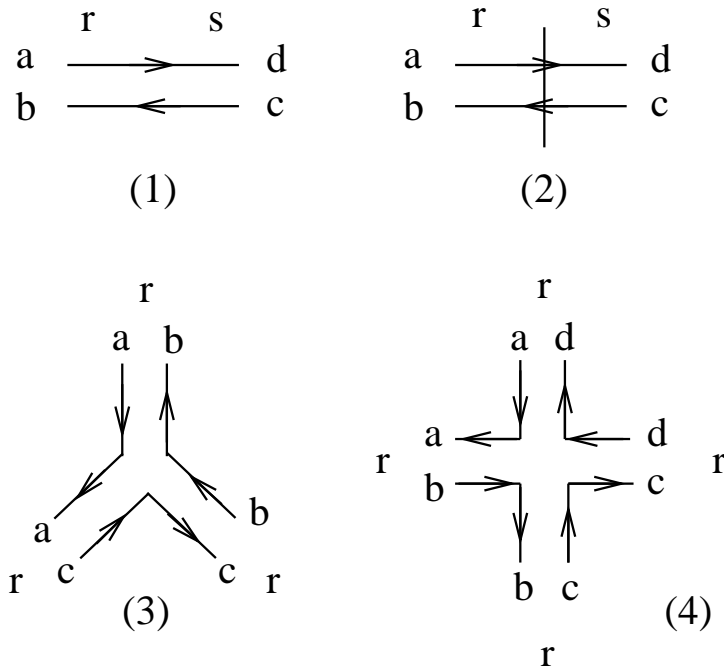


Figure 11: Feynman rules for the real time formulation of large N gauge theories at finite temperature: (1) is the temperature independent part of the propagator (5.44), while (2) is the temperature dependent part (5.45). The temperature dependent part of the propagator (2) is drawn with a “cut” line (the vertical line in the figure). The interaction vertices (3),(4) are drawn schematically, just to show the index flow structure. The interaction vertices do not mix the type-1 fields with the type-2 fields.

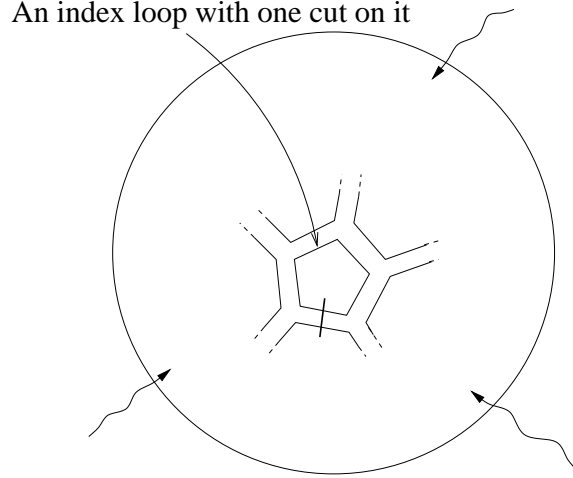


Figure 12: A 't Hooft-Feynman diagram with an index loop with only one cut on it.

to closed string states in the AdS-CFT correspondence. Throughout this section we will work in the planar limit $g \rightarrow 0$, $N \rightarrow \infty$ with the 't Hooft coupling $g^2 N$ fixed. In the planar limit, one can always associate a loop momentum to an index loop, as will be explained below.³¹ The total momentum on a propagator is a sum of two momenta associated with the index lines (taking into account the sign indicated by the arrows), and an external momentum flow if there is any. By a shift of loop momenta, which are integration variables, one can choose any tree sub-diagram connecting the external legs to express the external momentum flow. But once it is chosen, the integrations over loop momenta should be done with that fixed external momentum flow.

We first consider Feynman diagrams which have at least one index loop containing only one cut (which is denoted as a_i below). In this case the cut must be either 1-1 or 2-2 cut.³² By a shift of loop momenta, without loss of generality one can draw the flow of the external momentum without crossing the cut. From (5.45), the diagram with the 1-1 or 2-2 cut is proportional to a factor

$$\sum_{a_i=1}^N \frac{1}{e^{|\beta(p_{0i}-p_{0j})+2\pi i \frac{a_i-a_j}{N}|_R} - 1}. \quad (5.48)$$

Here, i, j label the index-momentum loops. As mentioned earlier, the loop momentum p_{0i} is “associated” with the gauge index a_i , that means, they always appear in the combination

³¹There are $\ell + 1$ index loops for ℓ (momentum) loop planar diagrams of a correlation function of gauge invariant operators, but one summation over gauge indices decouples since the gauge indices always appear as a difference of two indices [14, 45].

³²When there is a 1-2 cut on an index loop, there must be a 2-1 cut on that index loop.

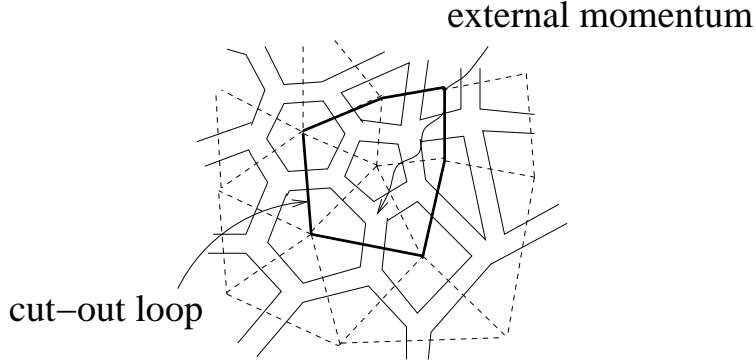


Figure 13: A cut-out loop on the dual graph of a 't Hooft-Feynman diagram.

$\beta p_{0i} + 2\pi i \frac{a_i}{N}$. The origin of this combination is the covariant derivative for adjoint fields. Therefore, by taking the background gauge around the field configuration (5.25), even when there are derivative couplings the loop momentum and the associated index also appear in the same combination. Such derivative couplings give rise to a multiplicative factor which is polynomial in $\beta p_{0i} + 2\pi i \frac{a_i}{N}$. Those just require a minor modification in the following discussions and do not change the conclusion about whether a diagram vanishes or not. Therefore, to keep the essential points clear in the presentation, we will only write down the formula for the case in which such derivative couplings are absent. Since we are working in the strict $N \rightarrow \infty$ limit, the sum over the gauge indices a_i can be replaced by the integral: $\frac{a_i}{N} \rightarrow \theta_i$, $\sum_{a_i=1}^N \rightarrow N \int_0^1 d\theta_i$. (To avoid repetition, this replacement will be implicit in what follows.) Then, one can Fourier expand the integrand of (5.48) as

$$\begin{aligned} \int_0^1 d\theta_i \frac{1}{e^{|\beta(p_{0i}-p_{0j})+2\pi i(\theta_i-\theta_j)|_R} - 1} &= \int_0^1 d\theta_i \sum_{n=1}^{\infty} e^{-n|\beta(p_{0i}-p_{0j})+2\pi i(\theta_i-\theta_j)|_R} \\ &= 0. \end{aligned} \quad (5.49)$$

From the definition (5.46), this kind of diagram has either all negative (when $p_{0i} > p_{0j}$) or all positive (when $p_{0i} < p_{0j}$) powers of $e^{2\pi i\theta_i}$. In either case, (5.49) vanishes. *Eq.(5.49) is the basic equation relevant for selecting the non-vanishing Feynman diagrams in the confined phase.*

The above vanishing mechanism means that if there is a cut “coming into” a face, there must be another cut “going out”. More precisely, it gives a conservation law for the phases ($2\pi\theta_i$ in (5.49)) at a face of the diagram, or a vertex in the dual graph. Thus in general, on the surviving diagrams those cuts must make up closed circuits on the dual graph (Fig.13). We have connected the starting and end points of the cuts on the same face of the diagram, because those faces are to be “filled” to make up closed string

worldsheet. Those closed circuits divide the worldsheet into regions which do not contain further cuts, otherwise the diagram will vanish (Fig.14). One can regard those closed circuits as made of “cut-out loops” [15]. For a closed string interpretation to be valid, the temperature dependence should appear in this way, since if the temperature dependence appears without making a closed loop on the diagram, it means that we are not just seeing the closed string but rather its sub-structure. (However, this is a description based on the expansion around the AdS geometry in the bulk. As we have seen in the previous section in the Euclidean case, in order for the closed string interpretation to be valid, the temperature dependence should be absorbed into the change of geometry in the bulk space-time.) One can show that the external momentum flow must cross the cut-out loop [15]. Since the external momentum flow can be drawn on a tree sub-diagram of the ’t Hooft-Feynman diagram, each cut-out loop can be associated with an edge of the closed string tree diagram (Fig.15). This indicates that the ’t Hooft-Feynman diagrams of the Yang-Mills theory at finite temperature in the confined phase give rise to closed string Feynman diagrams in a closed string field theory in the real time formalism.

One can also show that the cut has a correct energy dependence to be identified with a cut in the closed string field theory propagator in the real time formalism [15].³³ This is what the cuts in the picture should actually mean. The energy dependence of the cut in general has a form of eq.(5.45) without the gauge index dependent phase factor which is specific to our model, as one can see from the generality of the derivation.

Furthermore, we see that the propagator and interaction vertices ($\times i$) of the type-2 string fields of this hypothetical closed string field theory are complex conjugate of those of type-1. This is the property that in general field theory in the real time formalism should satisfy, see eqs.(5.44), (5.45),³⁴ and (5.47). The surviving ’t Hooft-Feynman diagrams are divided into regions inside which there’s no more cut (otherwise it vanishes as we have seen). Since the cut is the only temperature dependent part, this means that each region probes the same geometry as the original zero-temperature theory. Since type-1 fields and type-2 fields mixes only through the cuts, each region contains either only type-1 propagators and interaction vertices or those of only type-2. For every diagram with a region made of type-2, there must be a corresponding diagram with all propagators and vertices in that region are replaced by those of type-1 (Fig.16). This leads to the conclusion that the type-2 propagators and vertices of closed string field theory is complex

³³It was shown in the free field limit but expected to hold for finite coupling.

³⁴Again, the gauge index dependent phases in eq.(5.45) are specific to our gauge theory model and usually do not appear, and cancel in the surviving diagrams in the confined phase as we have seen.

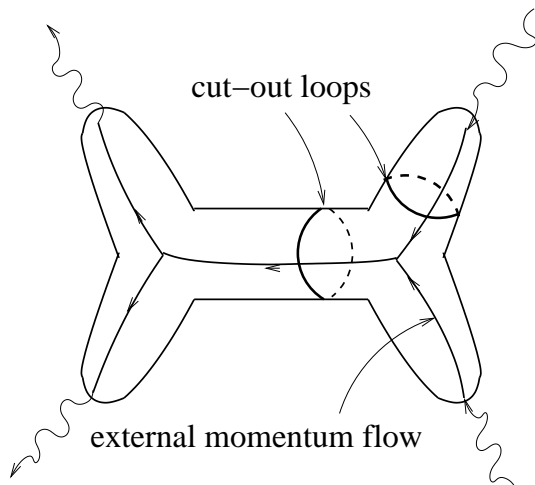


Figure 14: A ‘t Hooft-Feynman diagram identified with a closed string worldsheet. The cut-out loop must cross the tree sub-diagram where the external momentum flows. Thus the cut-out loop can be identified with the cut on a closed string propagator.

conjugate of those of type-1.

Thus, the dual description of the Yang-Mills theory in the confined phase can be consistently identified with *the closed string field theory at finite temperature in the real time formalism whose target space is the same as that of the zero-temperature theory*.³⁵ The field contents and the target space geometry in the bulk, obtained from the Yang-Mills side, are all uplifted from those obtained from the Yang-Mills theory at zero-temperature, just like in the standard real time formulation of field theory at finite temperature. This can be regarded as a Lorentzian version of the large N reduction. The point is that one can use most of the results in the zero-temperature also at finite temperature in the confined phase. If our understanding of the AdS-CFT correspondence at zero-temperature becomes more precise, so as the case at finite temperature in the confined phase.

³⁵The main reason we used string “field” theory here is that the worldline/worldsheet formulation of finite temperature field theory in the real time formalism is not developed enough. However, see [80] for some investigation of the first-quantized approach. We do not intend to pursue the non-perturbative analysis, which was one of the motivations in the construction of string field theory. We are just comparing the perturbative diagrams we would obtain from the field theory.

cuts of the closed string propagators

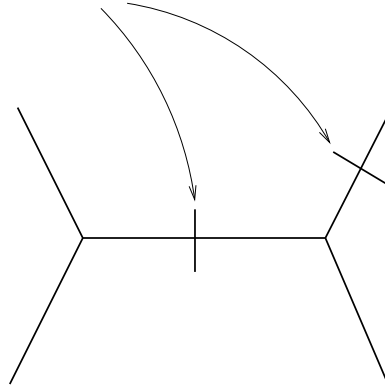


Figure 15: Fig.14 re-drawn as a closed string tree diagram in the real time formalism. The cut-out loops in Fig.14 are identified with the cuts on the closed string propagators.

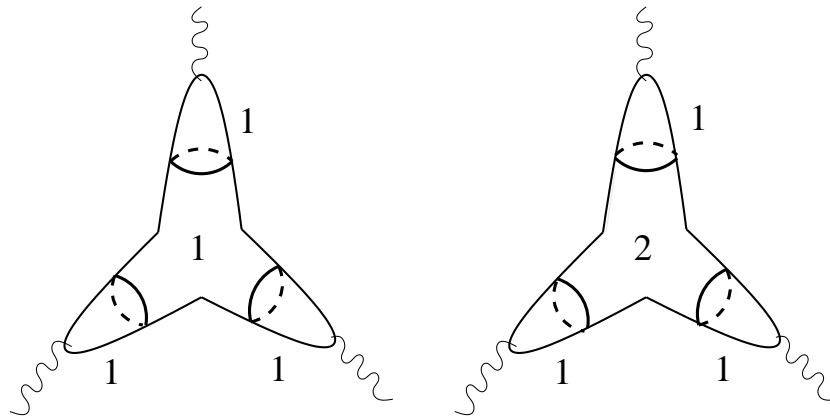


Figure 16: 't Hooft-Feynman diagrams divided into type-1 regions and type-2 regions by the cut-out loops. The type-2 region in the diagram on the right is complex conjugate to the corresponding type-1 region in the diagram on the left.

5.6 Comments on the deconfined phase and the black hole geometry

One might have had an impression that the structure of the bulk space-time are very different in the confined phase and the deconfined phase, because the one has a black hole and the other does not. This is correct, but we should also point out the similarity in the two descriptions. As one can see from the derivation of the path integral formulation of the real time formalism, one can either regard the real time formulation in AdS as two kinds of fields living in the same AdS, or instead the same fields living in two copies of AdS ((I) and (II) in Fig.17). In a similar way, in the black hole phase one can regard the fields to live on copies region I and region II in Fig.18. Although in the maximally extended AdS-Schwarzschild geometry these regions are connected through the region inside the black hole (the upper and lower triangle regions containing the singularity in Fig.8.³⁶), the Yang-Mills theory does not see these region, at least in a naive way,³⁷ because the boundary time corresponds to the asymptotic static observer's time which does not cross the horizon (see Fig.18). If one looks at only the region (I) and (II) in Fig.18, one may recognize that for the asymptotic observer it is the same real time formalism applied to the different geometries, i.e. the AdS geometry and the black hole geometry. Recall that the vertical parts of the contour which we sent to $t = \pm\infty$ put boundary conditions for the propagator when we derived our perturbative Feynman rules.³⁸

In the deconfined phase, the non-singlet states which cannot be interpreted as closed

³⁶We have called the region (II) “behind” the horizon since when looked from the region (I) it is so, but it is outside the another horizon and hence it is “outside” the black hole.

³⁷Nevertheless researchers challenge for extracting the information inside the black hole. See e.g. [81, 71, 82] for such efforts. This may be possible if there is a black hole complementarity [83], but at the same time it might make the description inside the black hole redundant, especially if one regards CFT side more fundamental and the space-time concept in the bulk as emerging.

³⁸As we have mentioned in subsection 5.3, the time translation in the vertical part of the contour can be identified with the thermal vacuum in thermo-field dynamics. The thermal vacuum (5.2) in the deconfined phase should correspond to choosing the Hartle-Hawking vacuum which is obtained by time translation in the Euclidean section of the black hole geometry and is invariant under the isometry generated by ∂_t in the bulk [74]. (For a description of the Hartle-Hawking vacuum related the discussion here, see [84]. See e.g. [85] for a examination of the Hartle-Hawking vacuum in a physically realistic context.) This should be understood if one recalls that in the Hamiltonian formulation, AdS-CFT correspondence is a (conjectural) isomorphism between Hilbert spaces of closed string theory on AdS and boundary CFT. The thermo-field dynamics on the boundary should essentially be the dual of the Israel's description of Hawking radiation via the thermo-field dynamics [86].

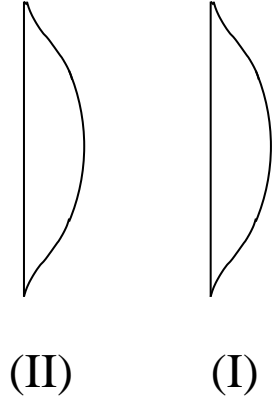


Figure 17: The Carter-Penrose diagram of the AdS space (I) and its copy (II).

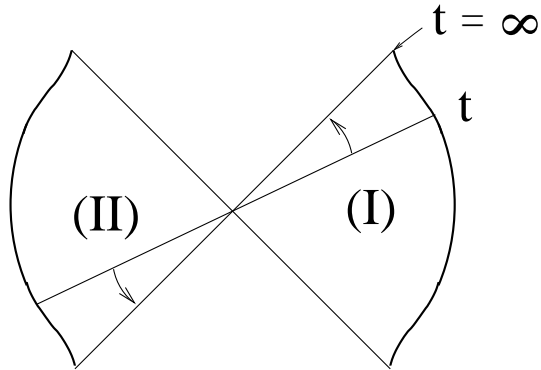


Figure 18: The Carter-Penrose diagram of the AdS-Schwarzschild black hole geometry with the asymptotic static observer time. The region inside the black hole (compare with Fig.8) is not reachable in finite asymptotic observer time t .

strings become important.³⁹ It is tempting to identify those non-singlet degrees of freedom with closed strings which look like open strings half hidden in the black hole horizon, but this interpretation requires further clarification.

It may be good to keep in mind that the appearance of the non-singlet states indicates that the bulk space-time picture probed by closed strings might be missing some important information of the bulk, especially about the black hole.

Acknowledgments

This note is based on talks presented at IPM String School and Workshop April 2006, Strings 2006 Shanghai Workshop and Hangzhou Workshop June as well as lectures delivered at ICTS-USTC March 2006 and at Chulalongkorn University April 2006. I would like to thank the organizers for the very nice workshops and the participants/attendants for stimulating discussions. I am also benefitted from the discussions at Strings 2006 Beijing and would like to thank for the support. I am also benefitted from my stay in NTNU and KIAS as well as visits to NCTS, NTU, CQUeST, Tokyo U.(Komaba), KEK, Osaka U. and Kyoto U.. I would like to thank D. Astefanesei, J. R. David, D. Ghoshal, K. Hashimoto, C. A. R. Herdeiro, T. Hirayama, P.-M. Ho, Y. Hosotani, N. Iizuka, D. P. Jatkar, S. Kalyana Rama, Y. Kazama, T. Kimura, A. Lawrence, K.-M. Lee, F.-L. Lin, H. Liu, J.-X. Lu, T. Matsuo, S. Naik, S. Nakamura, T. Nakatsu, J. Nishimura, B. Sathiapalan, E. Schreiber, G. W. Semenoff, A. Sen, M. Shigemori, S.-J. Sin, T. Takayanagi, S. Teraguchi, S. Terashima, D. Tomino, S. Wadia, P. Yi, K. P. Yogendran, T. Yoneya, A. Zamolodchikov and especially R. Gopakumar for useful discussions, explanations, comments and encouragements. I would also like to thank Ms. Ma, B. Ning, Z.-L. Wang, R.-J. Wu, M. Alishahiha, R. Fareghbal, M. M. Sheikh-Jabbari, Ms. Shirine, N. Salehirad, A. Chatrabhuti, R. Dhanawittayapol, A. Ungkitchanukit, P. Ittisamai, P. Karndumri, P. Patcharamaneepakorn, P. Wongjun, P. Kirduang, S. Sunanta, C.-C. Hsieh, F.-L. Lin, L.-L. Tsai, P. Chingangbam, S. Dutta, B.-H. Lee, H.j. Shin, S.-H. Yoon, S. Hu, S. G. Nibbelink, Ms. Shen, X. Xie, B. Zhao, S. S. Deshingkar, N. Mahajan, A. K. Ray, and many students, postdocs, professors, secretaries, local assistants and friends whose names I could not list here for warm hospitality and kind help. Last but not least, I would like to thank all the friends in my home institute for their continuous support.

³⁹See [87] for a study of a non-singlet sector in a two-dimensional model in the Lorentzian signature.

References

- [1] J. M. Maldacena, “The large N limit of superconformal field theories and supergravity,” *Adv. Theor. Math. Phys.* **2** (1998) 231–252, hep-th/9711200.
- [2] O. Aharony, S. S. Gubser, J. M. Maldacena, H. Ooguri, and Y. Oz, “Large N field theories, string theory and gravity,” *Phys. Rept.* **323** (2000) 183–386, hep-th/9905111.
- [3] B. Sundborg, “The Hagedorn transition, deconfinement and N = 4 SYM theory,” *Nucl. Phys.* **B573** (2000) 349–363, hep-th/9908001.
- [4] A. M. Polyakov, “Gauge fields and space-time,” *Int. J. Mod. Phys.* **A17S1** (2002) 119–136, hep-th/0110196.
- [5] O. Aharony, J. Marsano, S. Minwalla, K. Papadodimas, and M. Van Raamsdonk, “The Hagedorn / deconfinement phase transition in weakly coupled large N gauge theories,” *Adv. Theor. Math. Phys.* **8** (2004) 603–696, hep-th/0310285.
- [6] O. Aharony, J. Marsano, S. Minwalla, K. Papadodimas, and M. Van Raamsdonk, “A first order deconfinement transition in large N Yang- Mills theory on a small S^3 ,” *Phys. Rev.* **D71** (2005) 125018, hep-th/0502149.
- [7] R. Gopakumar, “From free fields to AdS,” *Phys. Rev.* **D70** (2004) 025009, hep-th/0308184.
- [8] R. Gopakumar, “From free fields to AdS. II,” *Phys. Rev.* **D70** (2004) 025010, hep-th/0402063.
- [9] R. Gopakumar, “From free fields to AdS. III,” *Phys. Rev.* **D72** (2005) 066008, hep-th/0504229.
- [10] R. Gopakumar, “Free field theory as a string theory?,” *Comptes Rendus Physique* **5** (2004) 1111–1119, hep-th/0409233.
- [11] O. Aharony, Z. Komargodski, and S. S. Razamat, “On the worldsheet theories of strings dual to free large N gauge theories,” *JHEP* **05** (2006) 016, hep-th/0602226.
- [12] J. R. David and R. Gopakumar, “From spacetime to worldsheet: Four point correlators,” hep-th/0606078.

- [13] I. Yaakov, “Open and closed string worldsheets from free large N gauge theories with adjoint and fundamental matter,” hep-th/0607244.
- [14] K. Furuuchi, “From free fields to AdS: Thermal case,” Phys. Rev. **D72** (2005) 066009, hep-th/0505148.
- [15] K. Furuuchi, “Confined phase in the real time formalism and the fate of the world behind the horizon,” Phys. Rev. **D73** (2006) 046004, hep-th/0510056.
- [16] S. W. Hawking and D. N. Page, “THERMODYNAMICS OF BLACK HOLES IN ANTI-DE SITTER SPACE,” Commun. Math. Phys. **87** (1983) 577.
- [17] E. Witten, “Anti-de Sitter space and holography,” Adv. Theor. Math. Phys. **2** (1998) 253–291, hep-th/9802150.
- [18] E. Witten, “Anti-de Sitter space, thermal phase transition, and confinement in gauge theories,” Adv. Theor. Math. Phys. **2** (1998) 505–532, hep-th/9803131.
- [19] G. W. Gibbons and S. W. Hawking, “ACTION INTEGRALS AND PARTITION FUNCTIONS IN QUANTUM GRAVITY,” Phys. Rev. **D15** (1977) 2752–2756.
- [20] S.-J. Rey and J.-T. Yee, “Macroscopic strings as heavy quarks in large N gauge theory and anti-de Sitter supergravity,” Eur. Phys. J. **C22** (2001) 379–394, hep-th/9803001.
- [21] J. M. Maldacena, “Wilson loops in large N field theories,” Phys. Rev. Lett. **80** (1998) 4859–4862, hep-th/9803002.
- [22] S.-J. Rey, S. Theisen, and J.-T. Yee, “Wilson-Polyakov loop at finite temperature in large N gauge theory and anti-de Sitter supergravity,” Nucl. Phys. **B527** (1998) 171–186, hep-th/9803135.
- [23] A. Brandhuber, N. Itzhaki, J. Sonnenschein, and S. Yankielowicz, “Wilson loops in the large N limit at finite temperature,” Phys. Lett. **B434** (1998) 36–40, hep-th/9803137.
- [24] G. W. Semenoff and K. Zarembo, “Wilson loops in SYM theory: From weak to strong coupling,” Nucl. Phys. Proc. Suppl. **108** (2002) 106–112, hep-th/0202156.
- [25] R. Rohm, “SPONTANEOUS SUPERSYMMETRY BREAKING IN SUPERSYMMETRIC STRING THEORIES,” Nucl. Phys. **B237** (1984) 553.

- [26] A. Sen, “Tachyon condensation on the brane antibrane system,” *JHEP* **08** (1998) 012, hep-th/9805170.
- [27] S. Kalyana Rama and B. Sathiapalan, “The Hagedorn transition, deconfinement and the AdS/CFT correspondence,” *Mod. Phys. Lett.* **A13** (1998) 3137–3144, hep-th/9810069.
- [28] J. L. F. Barbon and E. Rabinovici, “Closed-string tachyons and the Hagedorn transition in AdS space,” *JHEP* **03** (2002) 057, hep-th/0112173.
- [29] J. L. F. Barbon and E. Rabinovici, “Remarks on black hole instabilities and closed string tachyons,” *Found. Phys.* **33** (2003) 145–165, hep-th/0211212.
- [30] J. L. F. Barbon and E. Rabinovici, “Touring the Hagedorn ridge,” hep-th/0407236.
- [31] J. McGreevy and E. Silverstein, “The tachyon at the end of the universe,” *JHEP* **08** (2005) 090, hep-th/0506130.
- [32] G. T. Horowitz and E. Silverstein, “The inside story: Quasilocal tachyons and black holes,” *Phys. Rev.* **D73** (2006) 064016, hep-th/0601032.
- [33] K. Furuuchi, “Matrix model for Polyakov loops, string field theory in the temporal gauge, and winding string condensation in anti-de Sitter space,” hep-th/0608108.
- [34] T. Harmark and M. Orselli, “Matching the Hagedorn temperature in AdS/CFT,” *Phys. Rev.* **D74** (2006) 126009, hep-th/0608115.
- [35] O. Aharony and E. Witten, “Anti-de Sitter space and the center of the gauge group,” *JHEP* **11** (1998) 018, hep-th/9807205.
- [36] D. J. Gross and E. Witten, “POSSIBLE THIRD ORDER PHASE TRANSITION IN THE LARGE N LATTICE GAUGE THEORY,” *Phys. Rev.* **D21** (1980) 446–453.
- [37] S. Wadia, “A STUDY OF U(N) LATTICE GAUGE THEORY IN TWO-DIMENSIONS,”. EFI-79/44-CHICAGO.
- [38] S. R. Wadia, “N = infinity PHASE TRANSITION IN A CLASS OF EXACTLY SOLUBLE MODEL LATTICE GAUGE THEORIES,” *Phys. Lett.* **B93** (1980) 403.

- [39] K. Furuuchi, E. Schreiber, and G. W. Semenoff, “Five-brane thermodynamics from the matrix model,” hep-th/0310286.
- [40] G. W. Semenoff, “Matrix model thermodynamics,” hep-th/0405107.
- [41] L. Alvarez-Gaume, C. Gomez, H. Liu, and S. Wadia, “Finite temperature effective action, AdS(5) black holes, and 1/N expansion,” Phys. Rev. **D71** (2005) 124023, hep-th/0502227.
- [42] G. ’t Hooft, “A PLANAR DIAGRAM THEORY FOR STRONG INTERACTIONS,” Nucl. Phys. **B72** (1974) 461.
- [43] M. Brigante, G. Festuccia, and H. Liu, “Inheritance principle and non-renormalization theorems at finite temperature,” Phys. Lett. **B638** (2006) 538–545, hep-th/0509117.
- [44] T. Eguchi and H. Kawai, “REDUCTION OF DYNAMICAL DEGREES OF FREEDOM IN THE LARGE N GAUGE THEORY,” Phys. Rev. Lett. **48** (1982) 1063.
- [45] K. Furuuchi, “Large N reductions and holography,” Phys. Rev. **D74** (2006) 045027, hep-th/0506183.
- [46] V. L. Berezinski Ph.D Thesis (1970).
- [47] V. L. Berezinsky Sov. Phys. JETP **34** (1972) 610.
- [48] J. M. Kosterlitz and D. J. Thouless, “Ordering, metastability and phase transitions in two- dimensional systems,” J. Phys. **C6** (1973) 1181–1203.
- [49] A. M. Polyakov, “GAUGE FIELDS AND STRINGS,” CHUR, SWITZERLAND: HARWOOD (1987) 301 P. (CONTEMPORARY CONCEPTS IN PHYSICS, 3).
- [50] J. J. Atick and E. Witten, “THE HAGEDORN TRANSITION AND THE NUMBER OF DEGREES OF FREEDOM OF STRING THEORY,” Nucl. Phys. **B310** (1988) 291–334.
- [51] B. Sathiapalan, “VORTICES ON THE STRING WORLD SHEET AND CONSTRAINTS ON TORAL COMPACTIFICATION,” Phys. Rev. **D35** (1987) 3277.

- [52] Y. I. Kogan, “VORTICES ON THE WORLD SHEET AND STRING’S CRITICAL DYNAMICS,” *JETP Lett.* **45** (1987) 709–712.
- [53] V. Kazakov, I. K. Kostov, and D. Kutasov, “A matrix model for the two-dimensional black hole,” *Nucl. Phys.* **B622** (2002) 141–188, hep-th/0101011.
- [54] S. Alexandrov and V. Kazakov, “Correlators in 2D string theory with vortex condensation,” *Nucl. Phys.* **B610** (2001) 77, hep-th/0104094.
- [55] S. Alexandrov, “Matrix quantum mechanics and two-dimensional string theory in non-trivial backgrounds,” hep-th/0311273.
- [56] D. J. Gross and I. R. Klebanov, “Vortices and the nonsinglet sector of the $c = 1$ matrix model,” *Nucl. Phys.* **B354** (1991) 459–474.
- [57] D. J. Gross and I. R. Klebanov, “ONE-DIMENSIONAL STRING THEORY ON A CIRCLE,” *Nucl. Phys.* **B344** (1990) 475–498.
- [58] D. Boulatov and V. Kazakov, “One-dimensional string theory with vortices as the upside down matrix oscillator,” *Int. J. Mod. Phys.* **A8** (1993) 809–852, hep-th/0012228.
- [59] T. Suyama and P. Yi, “A holographic view on matrix model of black hole,” *JHEP* **02** (2004) 017, hep-th/0401078.
- [60] P. Basu and S. R. Wadia, “R-charged AdS(5) black holes and large N unitary matrix models,” *Phys. Rev.* **D73** (2006) 045022, hep-th/0506203.
- [61] K. Hori and A. Kapustin, “Duality of the fermionic 2d black hole and $N = 2$ Liouville theory as mirror symmetry,” *JHEP* **08** (2001) 045, hep-th/0104202.
- [62] J. McGreevy and H. L. Verlinde, “Strings from tachyons: The $c = 1$ matrix reloaded,” *JHEP* **12** (2003) 054, hep-th/0304224.
- [63] Y. Takahashi and H. Umezawa, “Thermo field dynamics,” *Collect. Phenom.* **2** (1975) 55–80.
- [64] H. Umezawa, H. Matsumoto, and M. Tachiki, “THERMO FIELD DYNAMICS AND CONDENSED STATES,”. Amsterdam, Netherlands: North-holland (1982) 591p.

- [65] G. W. Semenoff and H. Umezawa, “FUNCTIONAL METHODS IN THERMO FIELD DYNAMICS: A REAL TIME PERTURBATION THEORY FOR QUANTUM STATISTICAL MECHANICS,” Nucl. Phys. **B220** (1983) 196–212.
- [66] A. J. Niemi and G. W. Semenoff, “FINITE TEMPERATURE QUANTUM FIELD THEORY IN MINKOWSKI SPACE,” Ann. Phys. **152** (1984) 105.
- [67] N. P. Landsman and C. G. van Weert, “REAL AND IMAGINARY TIME FIELD THEORY AT FINITE TEMPERATURE AND DENSITY,” Phys. Rept. **145** (1987) 141.
- [68] M. LE BELLAC, “Thermal Field Theory,” Cambridge Univ. Pr. (1996) 256 p.
- [69] H. Umezawa, “Advanced field theory: Micro, macro, and thermal physics,” New York, USA: AIP (1993) 238 p.
- [70] I. Ojima, “GAUGE FIELDS AT FINITE TEMPERATURES: ’THERMO FIELD DYNAMICS’, KMS CONDITION AND THEIR EXTENSION TO GAUGE THEORIES,” Ann. Phys. **137** (1981) 1.
- [71] L. Fidkowski, V. Hubeny, M. Kleban, and S. Shenker, “The black hole singularity in AdS/CFT,” JHEP **02** (2004) 014, hep-th/0306170.
- [72] V. Balasubramanian, P. Kraus, A. E. Lawrence, and S. P. Trivedi, “Holographic probes of anti-de Sitter space-times,” Phys. Rev. **D59** (1999) 104021, hep-th/9808017.
- [73] G. T. Horowitz and D. Marolf, “A new approach to string cosmology,” JHEP **07** (1998) 014, hep-th/9805207.
- [74] J. M. Maldacena, “Eternal black holes in Anti-de-Sitter,” JHEP **04** (2003) 021, hep-th/0106112.
- [75] C. P. Herzog and D. T. Son, “Schwinger-Keldysh propagators from AdS/CFT correspondence,” JHEP **03** (2003) 046, hep-th/0212072.
- [76] R. Baier and A. Niegawa, “Analytic continuation of thermal N point functions from imaginary to real energies,” Phys. Rev. **D49** (1994) 4107–4112, hep-ph/9307362.
- [77] T. Banks, M. R. Douglas, G. T. Horowitz, and E. J. Martinec, “AdS dynamics from conformal field theory,” hep-th/9808016.

- [78] J. S. Schwinger, “Brownian motion of a quantum oscillator,” *J. Math. Phys.* **2** (1961) 407–432.
- [79] L. V. Keldysh, “Diagram technique for nonequilibrium processes,” *Zh. Eksp. Teor. Fiz.* **47** (1964) 1515–1527.
- [80] S. D. Mathur, “Is the Polyakov path integral prescription too restrictive?,” [hep-th/9306090](#).
- [81] P. Kraus, H. Ooguri, and S. Shenker, “Inside the horizon with AdS/CFT,” *Phys. Rev.* **D67** (2003) 124022, [hep-th/0212277](#).
- [82] G. Festuccia and H. Liu, “Excursions beyond the horizon: Black hole singularities in Yang-Mills theories. I,” *JHEP* **04** (2006) 044, [hep-th/0506202](#).
- [83] L. Susskind, L. Thorlacius, and J. Uglum, “The Stretched horizon and black hole complementarity,” *Phys. Rev.* **D48** (1993) 3743–3761, [hep-th/9306069](#).
- [84] T. Jacobson, “A Note on Hartle-Hawking vacua,” *Phys. Rev.* **D50** (1994) 6031–6032, [gr-qc/9407022](#).
- [85] R. M. Wald, “Quantum field theory in curved space-time and black hole thermodynamics,” *Chicago Univ. Pr.* (1994) 205 p.
- [86] W. Israel, “Thermo field dynamics of black holes,” *Phys. Lett.* **A57** (1976) 107–110.
- [87] J. M. Maldacena, “Long strings in two dimensional string theory and non- singlets in the matrix model,” *JHEP* **09** (2005) 078, [hep-th/0503112](#).